Nano Research
https://doi.org/10.1007/s12274-018-1980-5
Review Article
ISSN 1998-0124
CN 11-5974/O4

Magnetic labeling of natural lipid encapsulations with iron-based nanoparticles

Dewen Ye[1,2], Yan Li[1], and Ning Gu[1,2] (✉)

[1] *State Key Laboratory of Bioelectronics, Jiangsu Key Laboratory for Biomaterials and Devices, School of Biological Sciences & Medical Engineering, Southeast University, Nanjing 210096, China*
[2] *Collaborative Innovation Center of Suzhou Nano Science and Technology, Suzhou 215123, China*

Received: 14 November 2017
Revised: 31 December 2017
Accepted: 31 December 2017

KEYWORDS

magnetic labeling, iron-based nanoparticle (IBNP), natural lipid encapsulation(NLE), IBNP-membrane interactions

ABSTRACT

With superior biocompatibility and unique magnetic properties, iron-based nanoparticles (IBNP) are commonly encapsulated in cells and extracellular vesicles (EV) to allow for magnetic force controlled drug delivery and non-invasive tracking. Based on their natural source and similar morphology, we classify both cells and EVs as being natural lipid encapsulations (NLEs), distinguishing them from synthetic liposomes. Both their imaging contrast and drug effects are dominated by the amount of iron encapsulated in each NLE, demonstrating the importance of magnetic labeling efficiency. It is known that the membranes function as barriers to ensure that substances pass in and out in an orderly manner. The most important issue in increasing the cellular uptake of IBNPs is the interaction between the NLE membrane and IBNPs, which has been found to be affected by properties of the IBNPs as well as NLE heterogeneity. Two aspects are important for effective magnetic labelling: First, how to effectively drive membrane wrapping of the nanoparticles into the NLEs, and second, how to balance biosafety and nanoparticle uptake. In this review, we will provide a systematic overview of the magnetic labeling of NLEs with IBNPs. This article provides a summary of the applications of magnetically labeled NLEs and the labeling methods used for IBNPs. The review also analyzes the role of IBNPs physicochemical properties, especially their magnetic properties, and the heterogeneity of NLEs in the internalization pathway. At the same time, the future development of magnetically labeled NLEs is also discussed.

1 Introduction

Over the past few decades, studies aimed at understanding the relationship between cancer cells and stem cells have increased in number. Cancer cells are characterized by their ability to proliferate indefinitely, as well as their ability to destroy surrounding healthy cell tissues, whereas stem cells have gained attention because of their capacity for self-renewal and ability to differentiate into multiple cell types. In addition, stem cell transplantation has shown good therapeutic effects in regenerating damaged organs and tissues in numerous clinical situations including damage to the spinal cord, brain, and liver, as well as other organs [1, 2]. Numerous

Address correspondence to guning@seu.edu.cn

in-depth studies of tumor cells and stem cells have found that cell-derived microvesicles (MVs) are important in the ability of these cells to communicate with other cells. These extracellular vesicles (EVs) inherit a lipid membrane, nucleic acids, and proteins from their parental cells [3, 4], and are considered to be very attractive candidates for both diagnosis and treatment of disease due to their ability to allow cell content exchange through which the recipient cells can be altered [5]. Because of the closed spherical nature of both cells and EVs, they can encapsulate nanoparticles which allow them to be modified and targeted specifically, and so form an important research area in the nanotechnology field. Liposomes which can be synthesized *in vitro*, and have similar structures and surface properties, are also widely used as carrier platforms [6]. However, it has been reported that the natural membranes found in cells and EVs are almost an order of magnitude harder than synthetic liposomes [7–9]. In addition, they possess excellent biocompatibility, good durability, and a lower risk of malignant differentiation which are features that synthetic liposomes do not possess [8, 10]. Distinguished from synthetic liposomes, we classify both cells and cell-derived extracellular vesicles (EVs) as being natural lipid encapsulations (NLEs) because of their principal characteristics – i.e., the possession of natural lipid membranes.

Due to their unique magnetic properties and superior biocompatibility, iron-based nanoparticles (IBNPs) are more widely used in the field of nanomedicine than other inorganic nanoparticles (e.g., Au, Ag, Si) [11, 12]. A variety of nanoparticle preparation methods including chemical co-precipitation, sol-gel reactions, and a new method of using alternating magnetic fields (AMF) have been proposed previously by our laboratory [13]. IBNPs are commonly internalized into specific NLEs for use in both diagnostic and treatment applications. Compared with other inorganic materials, magnetically labeled NLEs can respond to external magnetic fields, which contributes to their unique biomedical applications. Based on their different magnetic responses, these applications include the following three aspects: (1) Magneto-mechanical forces and deformation generated by a gradient magnetic field [14–17], (2) magnetic hyperthermia caused by "local" heating under an alternating magnetic field [18, 19], and (3) MRI contrast agents which depend on spin for medical imaging [20–22].

There are two key challenges when labeling NLEs with IBNPs. One is how to improve the incorporation efficiency of the nanoparticles, and the other is to extend their retention time in NLEs without interfering with their performance [23]. Based on these considerations, new labeling methods are being developed to meet the requirements of high-speed, safety, and high iron content. The rationale for optimizing these labeling methods focuses primarily on the interaction between IBNPs and the natural bilayer membrane. Previous analyses have highlighted the importance of the physical properties of nanoparticles, but few studies have examined the effect of the type of NLEs on labeling efficiency [24]. Investigating the kinetics, thermodynamics, and signaling pathways involved in the interaction between nanoparticles and NLEs will have a significant impact on developing better strategies for the synthesis of nanoparticles and regulation of biological factors. This review summarizes the uses of magnetically labeled NLEs, and also discusses the labeling methods using IBNPs, analyzes the roles of the physicochemical properties of IBNPs, especially their magnetic properties, and describes the heterogeneity of NLEs in the internalization pathway. At the same time, the future development of magnetically labeled NLEs is also discussed.

2 Applications of magnetically labeled NLEs

The applications of magnetically labeled NLEs are primarily associated with the incorporated IBNPs. Due to their chemical stability, biocompatibility, and large surface that can be modified with a targeting molecule, the most promising application of IBNPs is to serve as a drug delivery platform for tissues containing lesions, especially tumors [25]. In this regard, a high affinity for the intended target cells, and site-specific accumulation at lesions are the most important aspects which must be evaluated, and therefore size, shape, and surface modification, which all have an impact on blood circulation time and targeting efficiency, need to be considered. In order to avoid the stochastic nature of ligand–receptor interactions, and difficulties in the control of drug release, stimulus-response systems

have been developed and are of significant interest [26]. By responding to changes in pH, temperature, and enzyme concentration, the release of drugs can be controlled both spatially and temporally. For systems containing IBNPs, once exposed to an alternating magnetic field (AMF), they will gradually produce heat through the Néel relaxation effect. This controlled release of heat can act as a switching signal that allows the drug to be administered at the desired location at the appropriate time, avoiding side effects in normal tissues [18, 27].

In addition to thermal properties, the magnetic force generated by a gradient magnetic field could alter the distribution of both IBNPs and labeled NLEs, whose distribution can be somewhat random after being injected *in vivo*. It has been suggested that an injected synthetic drug carrier containing IBNPs can be targeted to tumors with high accuracy and efficiency through the use of magnetic guidance [14, 28]. Furthermore, inspired by EV-mediated cell communication, Silva et al. separated EVs carrying IBNPs from THP-1 cells pre-treated with drug and IBNPs to target cancer cells, based on both magnetic guidance and strong EV attachment to the host cells, achieving a more accurate targeting to the cancer cells [29]. Importantly, depending on the exact location of the target site in the body, the spatial distribution of the magnetic field generated by the applied magnet can be altered to suit the particular need. In this regard, Tukmachev et al. have proposed a magnetic system consisting of two NdFeB magnets that are used to form a "trapping area" at the lesion site where magnetically-labeled stem cells tend to accumulate [30].

In addition to magnetic guidance *in vivo*, another promising biomedical application focuses on three-dimensional tissue engineering. In early applications, efforts have been devoted to design scaffolds to organize individual cells into various tissue shapes. Magnetically labeled cells offer the possibility of the construction of tissue engineering complexes without the need for a matrix. Based on the desired morphology of the tissue, cells can adopt a variety of shapes under the control of a magnetic field, including as sheets [31], spheroids [32], and tubular structures [33]. These basic shapes could then be further manipulated into any 3-D pattern. Whatley and coworkers have developed a prefabricated magnetic template that allows quick patterning of cell spheroids into desirable patterns [34].

As magnetic resonance imaging (MRI) contrast agents, IBNPs could also decrease the signal intensity in T_2- and T_2*-weighted magnetic resonance (MR) images by shortening T_2 and T_2* relaxation times after being magnetized by an external magnetic field. In addition to diagnosis of the disease site, tracking the movement of stem cells *in vivo* by MRI has recently become a very hot topic [35, 36]. As the role of EVs in the process of stem cell repair has gradually been confirmed, nanoscale vesicles will also need to visualized by MRI. However, this may be difficult, because recent data has shown that since EVs can be internalized by macrophages, allowing the IBNPs inside the EVs to enter into non-target cells would lead to false positive MRI signals [37]. In general, in order to achieve high quality imaging, two important properties must be considered, namely the magnetic properties of IBNPs and labeling efficiency. These important factors will be discussed in detail below.

3 Pathways for IBNP entry into NLEs

Approaches for internalizing nanoparticles into cells start with endocytosis. The basic labeling process is initiated by mixing nanoparticles in a biological environment such as blood or culture medium. Once nanoparticles make contact with the membrane surface, energy dependent internalization is triggered, after which the nanoparticles become enclosed within intracellular vesicles through a process of membrane bending and deformation. Depending on the interaction between nanoparticles and cells, the endocytic mechanism can been classified into four main different pathways, namely, phagocytosis, macro-pinocytosis, clathrin-mediated endocytosis, and caveolae-mediated endocytosis [38]. Phagocytosis is an actin-dependent pathway which is capable of eliminating dead cells, and is specifically used by phagocytic cells, such as macrophages, neutrophils, and dendritic cells [39, 40]. Different from the other pathways, macro-pinocytosis is the only mechanism by which cellular uptake of nanoparticles (0.2–5 μm) and fluids occurs without the need for receptors. During this process, the cytoskeleton is rearranged to allow the membrane to form a "C"

shaped ruffle that can trap fluids and micro-substances [41–43]. Clathrin/caveolae-mediated endocytosis is the most common pathway employed by cells, but requires the presence of clathrin/caveolae on the plasma membrane [24, 44]. Membranes invaginate into clathrin/caveolae-coated pits as a result of the coordinated assembly of proteins [45–47]. When nanoparticles enter into cells via the clathrin-mediated pathway they are usually transported to the lysosome where they ultimately undergo degradation; under some circumstances nanoparticles can escape this degradative fate [48, 49].

Such spontaneous endocytic processes are the theoretical basis for almost all of the emerging labeling techniques. Based on the fact that increasing the affinity between nanoparticles and membranes can promote membrane wrapping, strategies whereby the nanoparticle surface is modified with specific proteins or charged coatings have been proposed to increase the adhesion of IBNPs to membranes [50, 51]. In addition to endocytosis-based nanoparticle internalization, labeling approaches that do not rely on active cellular uptake are in widespread use, and are also suitable for labeling of EVs, including microinjection [52], electroporation [53], sonoporation [54], and magnetic field-mediated labeling [55, 56]. The methods used to promote cellular uptake are summarized in Table 1.

In addition to endocytosis, nanoparticles can also pass through membranes using physical force. Under these conditions, IBNPs can be driven into the NLEs by creating transient pores on the membrane surface; however, the excessive intensity of the stimulation required for pore formation may lead to irreversible damage to the membrane. Additionally, such approaches bypass the gradual transport of IBNPs through intracellular vesicles seen in the classical phagocytic process, and may result in altered fates and distribution of the IBNPs within the NLEs [54]. Based on the characteristics of the internalization pathway, endocytosis can therefore be classified as being either "active labeling", while the remaining four processes can be classified as being "facilitated labeling" (Fig. 1).

There is no doubt that labeling efficiency is vital for the successful application of magnetically labeled NLEs. It has been reported that intracellular iron loading above a certain threshold will result in loss of cell activity and function through the generation of increased levels of reactive oxygen species (ROS) in the cytoplasm [66, 67]. Thus, exploring new strategies to balance high iron content and biosafety remains a key issue for clinical application, and therefore requires a deeper understanding of the mechanism influenced by underlying factors.

4 Factors affecting IBNP labeling

It is generally believed that the physical and chemical properties of nanoparticles in terms of their size, shape, and surface modifications determine the extent of interaction between nanoparticles and the membrane of NLEs. In addition, the unique magnetic properties of IBNPs are also important factors. In this section, we systematically analyze the impact of the above factors on magnetic labeling of NLEs and the related mechanisms.

Table 1 Novel materials and processing methods in NLE labeling

Material	Cell/EV	Method	Effect	Ref.
Transferrin-MNP-MSN	U-87	Co-incubation	Encapsulation efficiency of 89.2 ± 1.1%	[57]
TAT-CLIO	hNSC	Co-incubation	Iron content up to 2.15 pg/cell	[58]
TAT- SPIO	Caco-2	Co-incubation	Fluorescence signal almost 5 times higher	[59]
Citrate-SPION	hMSC	Co-incubation	Iron content up to 69.6 ± 5.1 pg/cell	[60]
PLL-Ferumoxides	MSC	Co-incubation	Iron content up to 30.1 ± 3.7 pg/cell	[61]
Protein-Bound MNPs	HeLa	Pulsed magnetic field simulation	Iron content up to 7.6 pg/cell	[55]
MNPs	MDCK	Magnetic field simulation	MNPs are transported through cell barriers	[62]
Feridex	C17.2	Sonoporation	Iron content up to 10 pg/cell	[63]
Drug loaded $CoFe_2O_4$@$BaTiO_3$	SKOV-3	Electroporation	Uptake increased about 10%	[64]
Citrate-Fe_2O_3	Microparticle	Co-incubation	Microparticle can be detected by 1.5T MRI	[65]

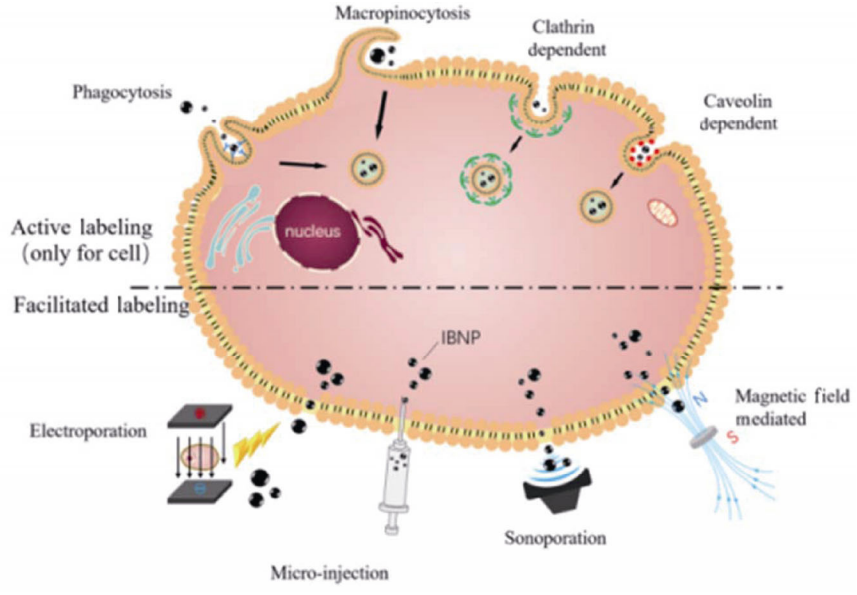

Figure 1 A schematic showing magnetic labeling of cells with IBNPs.

4.1 Shape and size

4.1.1 Shape

Numerous types of IBNPs with different sizes and shapes have been synthesized to meet the needs of a variety of applications. IBNPs can be molded into spheres, rods [68], worms [69], cubes [70], and ellipsoids [71]. Studies have been carried out to investigate the interactions between differently shaped IBNPs and the lipid membrane. It has been suggested that endocytic cellular uptake of rod-like IBNPs takes a longer time than that of spherical nanoparticles [71], which might arise as a result of differences in the length-to-width aspect ratio [68]. However, it has also been proposed that decreased cellular uptake can prolong the circulation time of drug carriers in blood vessels [72, 73]. Another recent study has shown that spheres may not be the most efficient shape for internalization. Brick shaped IBNPs have a 30-fold increase in uptake compared with sphere shaped IBNPs under an applied magnetic field [74].

4.1.2 Size

In addition to the shape effect, another dominant physical property of IBNPs which has been explored is size. Previous studies have suggested that size has a direct correlation with MRI contrast-enhancement [75–77]. The mass magnetization value under a 1.5T magnetic field increases from 25 to 102 emu/(g Fe), as the size of the Fe_3O_4 nanocrystals varies from 4 to 12 nm, a process referred to as a size-dependent MR signal [77]. This effect occurs on the nanometer scale where magnetic spins tend to be slightly tilted to form a disordered spin-glass-like surface layer, whereas normally spins are aligned parallel to the external magnetic field [78].

In addition to the intrinsic properties of IBNPs, the amount of IBNPs encapsulated in NLEs is another factor that determines the MR signal intensity of NLEs *in vivo*. What size range of IBNPs is most favorable for cellular uptake? What biophysical mechanisms are involved in the interaction between different sizes of IBNPs and bio-membrane? These issues have attracted the attention of more and more researchers. Scientifically, it is not reasonable to define the optimal size of IBNPs for all cells, because this depends on the cell type, or more precisely, the endocytic pathway employed to internalize nanoparticles differs in different cells. IBNPs with size over 100 nm can be readily phagocytosed by specialized phagocytic cells (e.g., macrophages) [79, 80]. Ultra-superparamagnetic iron oxide particles (USPIONs), with a size range of 30–100 nm, were used by Yu et al. to measure cellular uptake by macrophages. They showed that there was a positive correlation between nanoparticle size and internalization rate under conditions where the zeta potential values of all the samples

were the same [75]. These data showed a similar tendency to studies conducted by He et al. [81] and Mendes et al. [82]. Compared with smaller size IBNPs, larger IBNPs are more readily taken up by phagocytic cells, which may contribute to size-dependent hydrophobicity. As a result, the rapid recognition of large IBNPs (> 1 μm) by phagocytic cells allow nanoparticles with an ultra-small size to be "stealthy" and achieve prolonged circulation *in vivo* [83]. However, non-phagocytic cells are an exception on this rule. Sun et al. systematically investigated the effect of superparamagnetic iron oxide particles (SPIONs) (57 nm) and USPIONs (30 nm) on fibroblasts, progenitor cells, and HEP-G2-hepatoma cells, among other cell lines, and showed that SPIONs are preferred over USPIONs [84]. Another study has evaluated the size effect in MSCs; the uptake efficiency of IBNPs ranging from 60–160 nm decreased as the diameter increased [85]. These results indicate that sizes around 60 nm are more readily internalized, which is consistent with the study that showed that 30–60 nm seems to favorably involve the non-phagocytic pathway [86].

An understanding of how kinetics and force relate to receptor-mediated internalization could pave the way towards improving methods for the synthesis of nanoparticles [87]. A simple case can be considered, in which the uptake process is initiated without receptor binding, and the membrane bending force is the sum of three parts: Bending energy $C(\eta)$, stretching energy $\Gamma(\eta)$, and the additional deformation energy $\Lambda(\eta)$, where $\eta(0 \leqslant \eta \leqslant 1)$ is defined as the extent of wrapping [88].

First, defining the length scale λ as a characteristic to weigh bending and stretching energies, λ depends on the level of membrane tension σ and bending stiffness B

$$\lambda = \sqrt{\frac{2B}{\sigma}} \tag{1}$$

Under typical conditions, eigenvalues were given to σ and B, and it was found that 50 nm was a threshold less than which σ could be ignored, whereas beyond this size, σ cannot be ignored. For full wrapping of the NP ($\eta = 1$), $C = 8\pi B$ and stretching energy $\Gamma = 4\pi R^2\sigma$, where R is the nanoparticle diameter. To balance the stretching energy and adhesion energy ($4\pi R^2\alpha_{ns}$) where α_{ns} is the adhesion strength, R_{min} can be modeled as

$$R_{min} = \sqrt{\frac{2B}{\alpha_{ns} - \sigma}} \tag{2}$$

When taking receptor binding into account, some parameters can be altered in Eq. (2) and adhesion strength can be partitioned into two parts: enthalpic and entropic. R_{min} is represented as

$$R_{min} = \sqrt{\frac{2B}{\mu\xi_1 + \ln(\xi_0 / \xi_1)}} \tag{3}$$

ξ represents receptor density on the nanoparticles, ξ_1 (maximum density) and ξ_0 (density of remote region on the nanoparticles). According to equation, when R is below 5 nm, the deformation energy is not sufficient to warp the nanoparticles, and owing to the lack of receptors, this situation is referred to as "ligand-shortage", so ultra-small nanoparticles cannot drive the uptake process [86]. Molecular simulation has demonstrated, that for hydrophobic nanoparticles that could be spontaneously embedded in the membrane, the larger the nanoparticle, the more space they require to cross the bilayer membrane, and the more significant changes the membrane undergoes [89].

Besides the direct effects of size, size-induced changes due to modification of the IBNPs also have an effect on the interaction between membranes and NLEs. Gal et al. have shown that large-sized nanoparticles, arising as a result of high density poly (ethylene glycol) (PEG) grafting, had a decreased ability to interact with membranes, leading to low internalization of pre-coated IBNPs [90]. When IBNPs are introduced into biological systems, protein present in the serum

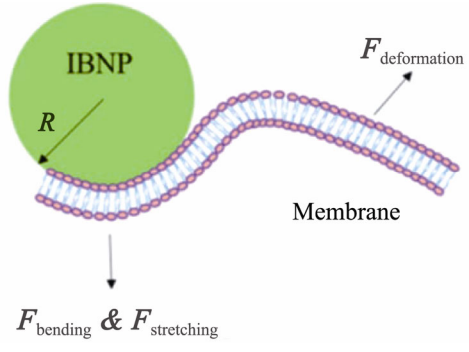

Figure 2 Membrane force diagram when wrapping IBNPs.

or the medium will be absorbed onto the surface of the nanoparticles. It has been shown that as the size of the nanoparticle increases, the type and amount of plasma proteins absorbed on the nanoparticles changes, and can have a further impact on the nanoparticle affinity for the membrane [91, 92].

IBNPs range in size from 5 to 200 nm for cell labeling, and so are not useful for relatively small EVs, which require ultra-small nanoparticles. Therefore, the importance of taking size into consideration should be emphasized before setting the desired goal.

Studies by Deserno et al. [88] and Yuan et al. [86] have shown that the optimal nanoparticle size calculated by mathematical modeling deviates from actual data. To achieve a better theoretical estimate, parameters such as chemical modification and shape of IBNPs should be included. Furthermore, the ideal model should be developed by continuously adjusting and fine tuning based on the experimental data.

4.2 Surface modification

Successful surface modification of IBNPs is crucial for their use in biomedical applications. These surface coatings can be classified according to their function, including (1) enhanced stability, (2) enhanced adhesion to NLE membranes, and (3) inclusion of drug molecules and reporter moieties to act as delivery vehicles [93, 94]. Here, we will elaborate on the first two aspects.

4.2.1 Stability enhancement

Naked IBNPs have a pH that is similar to human blood, which has been reported to induce crystal growth. Due to hydrophobic interactions between nanoparticles, they have a tendency to aggregate together to form clusters, and these aggregates exhibit ferromagnetic behavior, and further induce a greater degree of aggregation between clusters [95]. Aggregation of nanoparticles and dispersed homogeneous nanoparticles play different roles in the process of NLE labeling. Destabilization of nanoparticles caused by the presence of electrolytes and proteins in biological media have been reported to lead to overestimates of cellular uptake and cytotoxicity [96–98]. Destabilization of the dispersed IBNPs in the cell culture medium induces their sedimentation onto cell membranes, thus increasing their interaction with cells [97]. Since the aggregation of IBNPs may exacerbate their clearance by macrophages before reaching their target site, numerous polymers and inorganic substances have been used to coat the surface of IBNPs to form a stabilized shell which can increase their stability. Typical coatings include poly (ethylene glycol) (PEG) [99, 100], dextran [101], phospholipids [102], and SiO_2 [103]. The near-zero zeta potential and long chain structure of PEG allow it to adsorb little protein in the physiological environment, prolonging the circulation time, and reducing the likelihood of being recognized by the reticuloendothelial system [104, 105]. Other materials, such as horseradish peroxidase [106], arsenic acid [107], and poly(lactic-co-glycolic acid) [108] have also been developed to achieve higher colloidal stability.

4.2.2 Adhesion enhancement

As an ideal platform, IBNPs need to specifically target diseased tissues and cells. One of the strategies used is to conjugate small molecules and peptides that can specifically bind overexpressed proteins. These ligands are often modified on the membrane using a variety of conjugation chemistries. Carbonyl groups, amine groups, and sulfhydryl groups are broadly used to conjugate IBNPs with ligands through covalent reactions. The ligands can be classified into antibodies, peptides, and small molecules in descending order of size. They bind to receptors on the membrane in a targeted manner, causing membrane invagination at a local site, to trigger cellular uptake of the IBNPs through the typical endocytic pathways. Among these ligands, cell penetrating peptides that can translocate across cellular plasma membranes directly via non-receptor dependent and non-classical endocytosis, have shown remarkable efficiency in delivering gene therapeutic agents [109] and for drug delivery [110]. In addition to antibodies and peptides, recently, several studies have focused on using antibody fragments, or domains, to replace full length antibodies, including transferrin [111], affibodies [112] and neurotoxins [113].

In addition to using a specific protein as a target of interest, another promising targeting strategy relies on the stable and uniformly distributed charge on the membrane. The negatively charged cell membrane provides an electrostatic mechanism for nanoparticle binding. A number of studies have shown that charge

type and density are crucial parameters for the interaction between nanoparticles and cells. Osaka et al. [114] have employed both positively and negatively charged magnetic nanoparticles without any additional modification to investigate their uptake by breast cancer cells, and the data demonstrated a high affinity of cells for cationic nanoparticles. In general, compared with anionic nanoparticles, IBNPs with a high net positive charge are much more effective in interacting with bio-membranes through electrostatic attraction. Cationic materials such as poly-L-lysine (PLL) [115], protamine (PRO) [50], and polyetherimide (PEI) [51] have been used as transfection agents (TA) and have used extensively in stem cell labeling to obtain high levels of internalization efficiency [116]. Many studies have attempted to elucidate the mechanism of cellular uptake of cationic nanoparticles at the molecular level in order to develop strategies to enhance the adhesion of IBNPs to membranes. The mechanisms involved in the promotion of cellular uptake by cationic IBNPs can be summarized as follows. The first model is based on electrostatic forces that attract IBNPs to adhere to the membrane. When the attraction force is strong enough to drive the membrane to bend and enwrap the nanoparticle (Fig. 3(a)) this results in the generation of a bud that encapsulates the nanoparticle and subsequently transports it into cell [117].

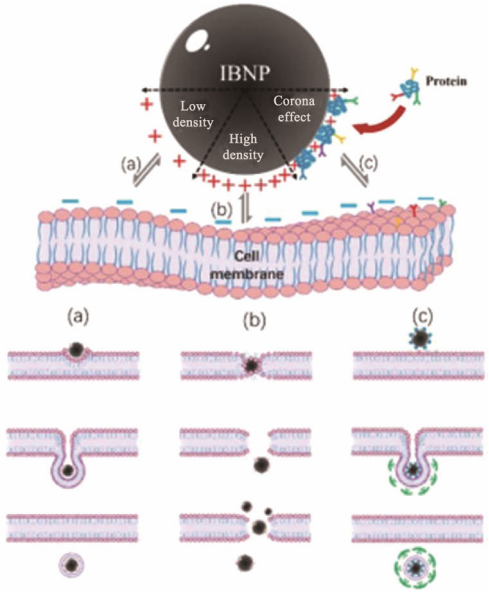

Figure 3 (a) Electrostatic adsorption effect. (b) Diffusion of IBNPs through transient pores. (c) Receptor mediated endocytosis by combination with protein on the corona.

In the second model, when the cationic terminal binds to the lipid membrane through electrostatic attractions, the membrane structure is changed and forms a pit to wrap the nanoparticle, after which the nanoparticle gradually enters the interior of the bilayer. Defective areas showing the disruptive pores have been observed through the use of a coarse-grained model. Furthermore, the higher the charge density, the more damage to the membrane occurs as a result of disruption [118]. Nangia et al. [119] have suggested that, upon the positive charge adhering to the membrane, the adhesion destroys the charge distribution equilibrium across the cell membrane. Li and coworkers [120] added nanoparticles to a giant unilamellar vesicle (GUV) format suspension to investigate NP-membrane interactions. They observed that as the concentration of the added nanoparticles increased, protrusions that consisted of membrane and labeled nanoparticles could be observed emanating from the membrane, and the GUV started to shrink. Furthermore, it has also been estimated that the pore diameter ranges from 18–27 nm, about 1/3 to 1/2 of the nanoparticle hydrodynamic diameter [121]. Thus, some publications have suggested that pores formed on the membrane allowed nanoparticles to diffuse directly through defective areas containing a disruptive pore, instead of by endocytosis (Fig. 3(b)) [118, 122, 123]. Because natural bio-membranes have the capacity of repair transient pores resulting from damage caused by changes in membrane tension [123], doses of cationic nanoparticles below a certain cutoff level can balance labeling efficiency and maintain good biocompatibility. In summary, cationic nanoparticles act as a double-edged sword for biological application. High cationic levels result in toxic effect to the NLEs' structure, while this disruptive effect can be used against tumors [124] and bacterial pathogens [125].

In the third model, nanoparticle interface components that are truly in contact with the bio-membrane can be in their original unmodified form, but can also exist as a complex biomolecule layer of absorbed proteins, which is referred to as the protein corona. The protein corona is preferentially adsorbed to cationic particles for the reason that serum has a net negative charge [126]. The corona has also been suggested by some groups to contain a few positive sites that allow negative

IBNPs to bind [127, 128]. Since the zeta potential of IBNPs can be increased after incubation with the fetal bovine serum often found in cell culture medium, the protein corona is commonly referred to as a 'game changer' in the NP-membrane interaction [129]. In some cases, the protein corona has been reported to inhibit cellular uptake by neutralizing or masking the positive surface charge of cationic nanoparticles [130, 131]. However, it is not correct to assume that the protein corona is a complete hindrance to cellular uptake. Babič et al. [132] have suggested that the corona does not entirely block the site of cationic (PLL) ligands. As the PLL/iron oxide ratio increases, the adsorption of serum proteins reaches a plateau at ratio of 0.002. It has been speculated that below this ratio, PLL chains are in full contact with the nanoparticle surface, while a higher ratio causes additional PLL chains to float free in the medium and allowing them to combine electrostatically with the membrane. In addition, some absorbed proteins in the corona can specifically bind to receptors on the cell membrane, which is thought to be a third mechanism that facilitates the cellular uptake of cationic nanoparticles (Fig. 3(c)) [133]. Evidence of the relationship between the amount of protein adsorbed and uptake efficiency has also been obtained from an investigation of PEG-coated nanoparticles [100]. The presence of the PEG ligand affects the adsorption of plasma proteins. A decrease in protein levels on the surface of IBNPs leads to a lack of receptor binding sites on PEG chains, thus affecting their adhesion to bio-membranes [134]. Additionally, the type of absorbed protein has a distinct effect on cellular uptake. One clue is that nanoparticles pre-coated with ApoH promote the uptake process, whereas, in contrast, nanoparticles pre-coated with the apolipoproteins ApoA4 or ApoC3 showed the opposite effect [135]. It has also been suggested that cellular uptake by different types of cells is observed to be different in the presence of corona [136]. Therefore, the overall effect of cationic nanoparticles on the endocytic process is very complex, and is coordinated by a variety of biological factors.

Cationic sites on the plasma membrane are believed to have a relatively weak attraction for negatively charged nanoparticles, and such an electrostatic attractive force merely drives the nanoparticle to the bilayer surface, but does not cause embedding in the bilayer. Ayala et al. systematically examined the effect of carboxymethyl groups incorporated in the nanoparticle shell on uptake and colloidal stability. With measured surface zeta potentials ranging from –50 to 5 mV, the internalization by cells increased with enhanced negative surface charge [137]. Another study has also shown that the rate of internalization of anionic nanoparticles is less than that of cationic nanoparticles [138]. Moreover, neutrally charged particles tend to have the lowest uptake with the rank order of IBNP cellular uptake being: IBNPs (positive) > IBNPs (negative) > IBNPs (neutral) [139, 140]. Interestingly, a recent study has demonstrated that cells at different stages selectively employ endocytosis of nanoparticles with neutral, anionic, and cationic functionalities. Metastatic cancer cells more readily internalize nanoparticles with anionic surfaces, while late stage cells could be easily targeted with sulfonate functionalized nanoparticles [141]. Another study has shown that nanoparticle uptake by adipose-derived stem cells is reduced significantly with increased cell passage number [142]. When IBNPs with negatively charged surfaces are exposed to the biological environment, the anionic ligands attract and bind proteins. Fleischer et al. used a model system composed of IBNPs functionalized with either anionic or cationic groups to investigate the effect of protein layer on nanoparticle binding and internalization. They showed that BSA adsorption to cationic polystyrene nanoparticles was disrupted, causing the BSA–NP complexes to bind to scavenger receptors, whereas complexes on anionic IBNPs maintained their natural structure and bound to native albumin receptors [127].

Given that a charged surface may cause cell destruction, the density of the ligand should be adjusted to a rational level to balance efficiency and biosafety. Numerous types of pathway are involved in the labeling process and which pathway plays a dominant role has not been clarified. The amount of iron content per cell is decided by all of the potential uptake pathways, and even if there is an increase in iron content in cell, it may also be influenced by negative factors such as the masking effect of the corona.

4.3 Magnetic properties

Owing to the unique magnetic properties of IBNPs, the interaction between IBNPs and membrane can be

manipulated by various types of magnetic fields. This control relies on the fact that when a magnetic field is applied, the particles will be magnetized immediately as result of their arrangement of atoms, while the magnetism disappears immediately after the magnetic field is removed; such a characteristic is referred to as superparamagnetism [143]. The magnetic forces generated by a static magnetic field (SMF) [144], a pulsed magnetic field (PMF) [55], and an alternating magnetic field (AMF) [62] have been shown to be capable of increasing the cellular uptake of IBNPs. Since the initial study achieved rapid and efficient gene transfer of a SPION-DNA complex in the presence of a SMF, a process referred to as "magnetofection" [145], the effect of a SMF has received more and more attention. Commercially available permanent magnets are often placed under culture dishes to generate a relatively uniform SMF [146]. A systematic investigation into the mechanism has found that there are two main explanations behind the SMF effect: 1) Force dependence, 2) increased levels of endocytosis-associated protein. MacDonald et al. formulated magnetic nanoparticles with different magnetite loads to assess the influence of magnetic force on nanoparticle uptake. They found that the internalization rate depended on the magnetite levels within the particle, which reflected the magnetic force generated and which caused the nanoparticle to be pulled into contact with membrane surface [147]. This result was consistent with research conducted by Barnes et al. [148]. Under an SMF, in addition to the magnetic force-mediated physical effects, the expression of genes and proteins associated with the endocytosis process were also found to be regulated. Chaudhary et al. [149] examined the cellular uptake of IBNPs under a 350 mT SMF, and the published data showed that the clathrin levels in cells increased during stimulation. Cellular uptake was observed in the presence of endocytosis blockers, while the presence of an SMF could reverse this phenomenon. The authors proposed some probable mechanisms for this effect. First, over expression of clathrin to a certain extent overwhelmed the endocytosis blockers. Second, the magnetic force generated is strong enough to overcome the endocytosis blockers. The third possibility may be that the presence of the SMF initiates a different uptake pathway. Additionally, by investigating the factors involved in promoting uptake, it was suggested that the internalization enhancement effect seemed to be magnetic field and concentration-dependent, but was not associated with the processing time [144, 146]. In summary, SMF magnitudes in the range of 50–500 mT might be suitable to balance both labeling efficiency and biosafety.

The term PMF usually refers to a low-frequency, high-field narrow pulse magnetic field, through which fast labeling can be achieved within seconds. Lee et al. exerted a high-intensity PMF to label adherent HeLa cells with a magnetic field strength of 0.6 T, delivered three times at intervals of 6 s, and the amount of labeling was increased from 1.9 pg per cell to 7.6 pg per cell [55]. It has been suggested that the vibration of IBNPs under the PMF creates metastable cell membrane pores to facilitate the labeling process, and this mechanism has been described as 'magnetic bombardment' by observing the iron filings changing their position after one pulse [150, 151]. Considering that a PMF can induce an electric field, and based on the fact that a pulsed electric field can result in structural, protein, and charge changes and even pore formation on the membrane [152, 153], some studies have speculated that the promotion of endocytosis under a PMF might result from an altered charge distribution in the outer leaflet of the membrane which leads to irreversible cell membrane permeabilization [154, 155]. In addition to the enhancement of uptake, a PMF is also found to aid in transport of IBNPs across cell barriers by reducing the level of IBNP aggregation [62].

AMF is another type of magnetic field whose strength and direction change over time according to certain rules. When IBNPs are exposed to an AMF, an induced eddy current in the conductor generates heat and which propagates to the tissue. One study has shown that the hyperthermia transiently induces an increase in blood–brain barrier permeability within 0.5 h, without harm to cells, indicating that the heat generated by IBNPs plays a significant role in nanoparticle-cell interaction [62]. Recently, our group systematically investigated the effect of temperature on the asymmetric membrane of eukaryotic cells by simulating coarse-grained molecular dynamics, and these data revealed that high temperatures can accelerate the diffusion of nanoparticles by causing a disordering of phospholipids

[156].

Summarizing the labeling stimulated by magnetic fields, the whole process takes less time than utilizing transfection reagents, and does not induce biological toxicity to NLEs, but the increase in iron content per cell is not very large. So far, explanations underlying magnetic field induction mechanisms such as the "magnetic bombardment" theory are only based on the motion of IBMPs driven by external magnetic fields. This assumed potential non-endocytic pathway requires more analysis and verification of both cell membrane morphology and the entire labeling process.

5 Heterogeneity of NLEs in labeling

In addition to the effects caused by the physicochemical properties of IBNPs, the diversity of cells and EVs are not negligible factors. Although we classify them as NLEs because of their similarities in structure and origin, there are still significant differences in the labeling of cells and EVs, and different types of cells exhibit distinct labeling efficiencies [157, 158]. This section will focus on the analysis of intercellular heterogeneity and the differences in cell and EV labeling involved in magnetic labeling.

5.1 Cell type

For any given IBNP, a significant difference in cellular uptake efficiency has been observed in various cell types, confirming that cell type-dependent penetration is involved in IBNP-membrane interactions. It is known that these differences are determined by the physiology of each type of cell. Since it is impossible to make a universal assessment of all type of cells, we selected two kinds of cells: tumor cells and stem cells as models. Mailander et al. analyzed the iron content of labeled MSC and HeLa cells with two commercially available SPIOs (Resovist and Feridex) without TAs. For each group, the calculated iron content in the HeLa cancer cells was much higher than MSCs across the concentration gradient detected [157]. Perevedentseva et al. compared the internalization of A549 lung human adenocarcinoma cells with normal cells revealing that the level of internalized nanoparticles in cancer cells exceeded those in non-cancer cells [159]. Similar results were also observed by Gal et al. [158] and Srinivasan et al. [160]. Which factors lead to high endocytosis of nanoparticles by tumor cells? As we know, the main distinguishing characteristics of cancer cells are their strong proliferative ability and high invasiveness. Based on tumor cell research, we attempted to explore the possible mechanisms. Membrane proteins such as receptor tyrosine kinases (RTKs) and transferrin are essential for internalization, and these proteins need to be constantly recycled to the surface in order to provide essential energy and metabolites for proliferation [161, 162]. Importantly, the major proteins that mediate this continuous endocytic process are clathrin and caveolin, which also serve as the most important nanoparticle internalization-associated proteins. A study conducted by Bitsikas et al. [163] revealed that clathrin-mediated endocytosis is responsible for almost all of the molecules on the membrane. Additionally, it has been reported that down regulation of caveolin-1 caused increased expression of β-catenin, whereas decreasing the level of E-cadherin promoted the migration and invasive abilities of NCI-H460 cells [163]. These clues suggest that overexpression of these phagocytosis-related proteins favors the cellular uptake of special receptors and at the same time shows an enhancement of the cellular internalization of nanoparticles. Among the over expressed proteins in cancer cell lines, caveolin-1, an internalization-associated protein, was found to be up-regulated in a number of multidrug-resistant cancer cells including adriamycin-resistant MCF-7 AdrR breast adenocarcinoma cells, colchicine-resistant HT-29-MDR colon carcinoma cells, vinblastine resistant SKVLB1 ovarian carcinoma cells, and taxol resistant A549-T24 lung carcinoma cells [163, 164]. Sahay et al. exploited the different endocytic pathways in both normal and tumor cells, suggesting that in cancer cells internalization proceeds mainly through caveolae-mediated endocytosis [165]. By searching for changes in endocytic/trafficking proteins and actin regulators in the COSMIC (Catalogue of Somatic Mutations in Cancer) database, changes in both caveolin-1 and caveolin-3 have been found [166].

These changes in protein expression might be related to the nuclear structure. The nuclei of most normal cells have a regular and ellipsoid shape, but an irregular and folded nuclear contour is observed in most cancer cells (Fig. 4). Such a characteristic of cancer cells is

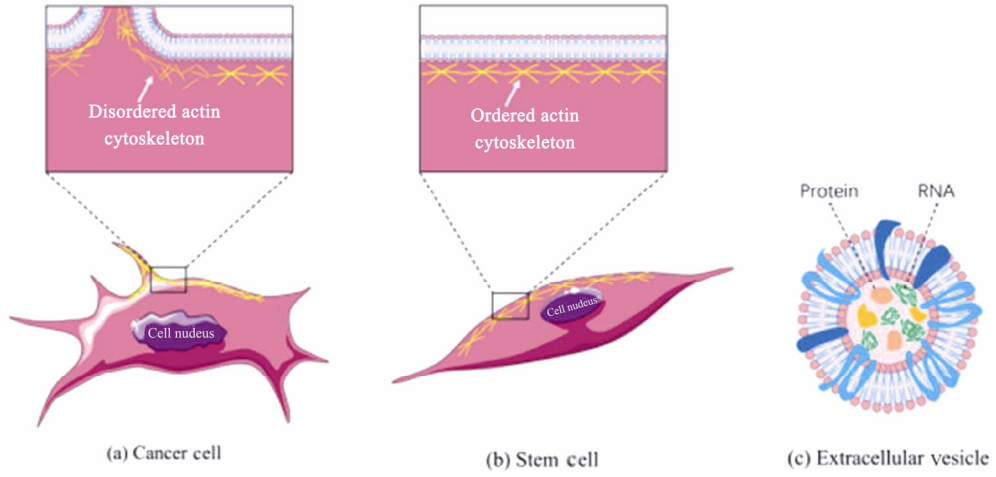

Figure 4 Comparison of cancer cells, stem cells, and extracellular vesicle morphology. (a) A folded nuclear shape and a disrupted cytoskeleton are observed in cancer cell. (b) For stem cells, they possess an ordered cytoskeleton and an elliptical nucleus. (c) Only protein and RNA inside the extracellular vesicles.

reported to have impact on chromatin organization and gene positioning [167]. This inspired us to think that an altered nuclear shape might affect gene expression patterns and lead to the expression of endocytosis-related proteins such as caveolin. In conclusion, we speculate that the transformation of normal cells to cancer cells is accompanied by the mutation of endocytosis-related proteins, leading to a high level of endocytosis and proliferation.

Besides the characteristics of infinite proliferation in cancer cells, another distinct feature of cancer cells is their rapid invasion capability. Structurally, there is evidence that the transformation of normal cells into cancer cells is characterized by disruption and reorganization of cytoskeleton, as well changes in the interaction of integrins [168]. Furthermore, an altered cytoskeleton is reported to make cancer cells more pliable than normal cells [169], and this decreased stiffness has been shown to be induced by disruption of actin filaments [168–171]. Upon remodeling of the actin cytoskeleton beneath the plasma membrane, the structure of filopodia and lamellipodia in cancer cells are visible [172] (Fig. 4(a)), whereas stem cells retain an ordered and intact cytoskeleton (Fig. 4(b)). Notably, the endocytosis-related protein, clathrin, has been found to be active in the migration of cancer cells. Elkhatib and coworkers, utilizing a fluorescence method, examined an invasive human breast cancer cell line that was prone to metastasize, and successfully demonstrated that clathrin-coated pits were attached to, and surrounded, collagen fibers. These clathrin-coated pits squeezed the collagen fibers, thereby increasing the grip strength of the cancer cells and allowing them to migrate further, so that clathrin-coated pits allowed about 50% of the cells to attach to the surrounding structures [173].

5.2 Extracellular vesicles

Similar to cells, the composition of the EV membrane comprises of membrane fusion proteins, tetraspannins, heat shock proteins, as well as lipid-related proteins [174, 175]. Cells are complex and contain organelles and nuclei, whereas EVs contain only proteins, miRNAs, and other non-coding RNAs (Fig. 4(c)). The substances inside the EVs determine the most fundamental difference between cells and EVs in the labeling process – EVs are not metabolically active, and thus cannot be defined as living biological entities [175]. Due to their lack of metabolic function, EVs cannot complete the entire process of external substance absorption, digestion, and excretion. Furthermore, for cells, apoptosis and toxicity are important factors to be considered for cells to maintain themselves, whereas for EVs, ensuring the integrity of their membrane structure is sufficient, and this makes them easier to handle than cells [176]. Additionally, IBNPs are digested in cell lysosomes resulting in the release of iron ions, further resulting in cytotoxicity and inducing cell apoptosis as a result of increased ROS levels [177], whereas EVs provide a safer space to store IBNPs [20]. Notably, restricted by the small size of EVs, only ultra-small superparamagnetic

iron oxide nanoparticles (USPIO, ≤ 10 nm) can be inserted into EVs [178]. Due to their inability to autonomously acquire nanoparticles in an extracellular medium, recently developed magnetic labeling techniques for EVs are discussed in this section.

EVs originate by the pinching off of membranes from endocytic vesicles. The EVs fuse with early endosomes, partially mature and then differentiate into late endosomes and multi-vesicular bodies (MVBs, a kind of late endosome), and then re-fuse with membrane, and are released into the extracellular environment as EVs [179, 180]. When IBNPs are incubated with parent cells, the internalized IBNPs have a certain chance of being transferred to the EVs, which enables "indirect" labeling of the nanoparticles (Fig. 5(a)). Busato et al. have proposed a method to obtain labeled exosomes while ensuring their biological function and membrane integrity, the protocol consists of two steps: 1) Incubating cells with IBNPs, 2) isolating labeled exosomes from the incubated cells. The presence of IBNPs was verified by the clear presence of a dark spot in the isolated exosomes by transmission electron microscope (TEM). Subsequent studies in rats demonstrated that the EVs were detectable, although the nanoparticle content in each exosome was extremely low [181, 182]. Another study demonstrated that macrophage-derived EVs labelled with IBNPs provide a promising way of being used as a drug delivery system to target cancer cells [29]. However, only a small fraction of the internalized nanoparticles will be encapsulated into EVs and secreted. This method of labeling has many uncontrollable factors that result in a low labeling efficiency, while direct labeling of separated EVs with IBNPs has been shown to be more efficient. Due to their lack of metabolic function, EVs cannot internalize IBNPs by co-incubation, despite the presence of receptor proteins embedded in the membrane. The technique of electroporation, through which pores of 1–10 nm can be instantaneously formed in membranes, enables nanomaterials to diffuse into EVs (Fig. 5(b)). For example, Zhao et al. [183] loaded nanoparticles efficiently into human oral squamous carcinoma (CAL27) cell-derived MVs by electroporation, conferring high-resolution and dual-mode tracking of MVs. The inevitable drawback of this approach is the damage to the membrane structure caused by the high intensity of the electric field used for electroporation, but the transient non-destructive pores can recover after 30 minutes incubation in the medium. With reference to optical tracing of fluorescent dyes attached to EVs [184], IBNPs modified with a specific protein can bind to a receptor on the membrane, allowing the membrane outer surface to be directly labeled with magnetic nanoparticles by simple co-incubation [65]. It is not yet certain whether such modifications of the membrane surface with nanoparticles, by occupying the receptor protein binding site will disturb the combination of recipient cells and EVs while activating the elimination of the immune system.

The unique ability of EVs to bind cells allow them to act as an intermediate, by which they can act as a drug delivery system capable of transferring the cargo to recipient cells. (Fig. 5(c)) [29, 185]. Zhu et al. have packaged RNA into MVs by electroporation, these pre-loaded MVs were then incubated with MDA-MB-231 cells for several hours after which the nanovector was

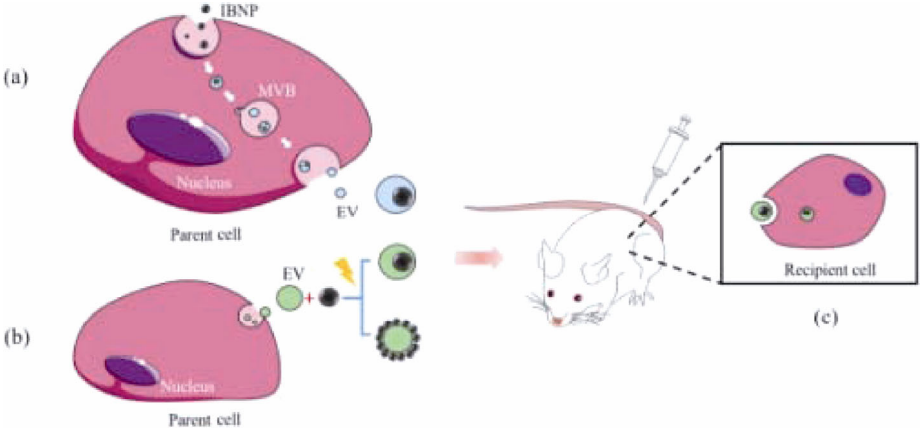

Figure 5 Labeling patterns of EVs. (a) Indirect label of EVs. (b) Direct label of EVs. (c) Re-labeling of recipient cells by EVs.

efficiently transported into cells [185]. In contrast to the cell membrane, abundant lipids in the EV membrane, such as sphingomyelin and desaturated lipids, endow it with a greater ability to resist degradation [186].

Understanding the mechanism of communication between EVs and recipient cells is the basis for further manipulation of the labeling and targeting processes. Phagocytosis seems to be the dominant pathway during the process of recipient cells internalizing EVs with inhibitors [187]. In another study by Nanbo et al. the caveolae-mediated endocytic pathway was employed in the internalization of secreted EVs from B cells by CNE-1 cells [188]. The binding of ligands to receptors has been proven to be mediated by membrane proteins such as heat shock proteins (HSPs) and Toll-like receptors [189, 190]. Based on the above data, efficient communication is mediated by multiple pathways. Compared with the modification of specific receptors on IBNPs, nanoparticle labeled EVs may offer a unique prospect for the magnetic labeling of target cells. It can be speculated that a high iron content per cell can be achieved by utilizing labeled EVs as the target recipient cells. The source and type of EVs have a great influence on labeling efficiency, and should be taken into account [5].

6 Summary and outlook

In this review, we summarize the magnetic labeling of NLEs, and provide a comprehensive description of labeling methods, as well as the interactions between NLE membranes and IBNPs affected by a series of factors. Endocytosis as an "active pathway" is a common route for the non-phagocytic internalization of IBNPs, whereas external force dependent internalization is classified as a "facilitated pathway". Since the encapsulation amount and the biological toxicity of IBNPs are determined by the IBNP-membrane interaction, two aspects (i.e., IBNP and NLE) should be taken into account. The size range within which IBNPs can be efficiently internalized is theoretically based on the balance between the limited membrane tension and attraction caused by receptor binding, and it differs between non-phagocytic and phagocytic cells. For commonly used charged TAs, protein-modified cationic nanoparticles can facilitate cellular uptake through electrostatic adsorption, disruptive pore formation, and receptor recognition. However, among these mechanisms, pore formation caused by high ligand density ligand is accompanied by biological toxicity, and absorbed proteins do not always have a positive effect. The increased anionic nanoparticle cellular uptake may stem from their stability in the medium and the protein corona formed on their surface. Compared with other inorganic nanoparticles, magnetic properties are unique to IBNPs, allowing a magnetic field to regulate the labeling process. Almost all types of magnetic fields have the potential to be applied to increase cellular uptake through the generated magnetic force, heating, and up-regulation of proteins level. So far, studies on magnetic field induction have not been comprehensive and convincing, which urges more investigation. In addition to the role of IBNPs, the labeling processes for metabolically inactive EVs and various cells are quite different, and these differences arise as a result of differences in structure and composition between EVs and cells, which reflect their unique function. Furthermore, in order to explain the high level of cellular uptake by cancer cells, we found some clues based on their up-regulated levels of caveolin and active clathrin which appear to be necessary for metastasis and invasion. Finally, we highlight the difference in magnetic labeling of EVs and cells.

The complexity of the properties and biological effects of IBNPs provides numerous challenges in investigating the interaction with IBNP-NLEs. So far, the investigation has progressed well, but the answers are not yet clear. The most important bottleneck remaining in the development of labeling for tracking and targeting is how to encapsulate nanoparticles as efficiently as possible without interfering with cell function, which appears to be difficult to balance because of limitations in cell number and their carrying capacity. However, EVs have drawn a great interest due to their advantages of being an abundant source, lack of metabolic function, and the ability to partially replace their own parent cells, and more effort should be devoted to achieving the maximum potential of EVs in the diagnostic and therapeutic areas.

Acknowledgements

This work was supported by the National Basic Research

Program of China (Nos. 2013CB733804 and 2013CB934400), the National Key Research and Development Program of China (No. 2017YFA0104301), the National Natural Science Foundation of China for Key Project of International Cooperation (No. 61420106012), and the Collaborative Innovation Center of Suzhou Nano Science and Technology (No. SX21400213).

References

[1] Lin, C. L.; Ho, Y. S. A bibliometric analysis of publications on pluripotent stem cell research. *Cell J.* **2015**, *17*, 59–70.

[2] Petrou, P.; Gothelf, Y.; Argov, Z.; Gotkine, M.; Levy, Y. S.; Kassis, I.; Vaknin-Dembinsky, A.; Ben-Hur, T.; Offen, D.; Abramsky, O. et al. Safety and clinical effects of mesenchymal stem cells secreting neurotrophic factor transplantation in patients with amyotrophic lateral sclerosis results of phase 1/2 and 2A clinical trials. *JAMA Neurol.* **2016**, *73*, 337–344.

[3] Yáñez-Mó, M.; Siljander, P. R. M.; Andreu, Z.; Zavec, A. B.; Borràs, F. E.; Buzas, E. I.; Buzas, K.; Casal, E.; Cappello, F.; Carvalho, J. et al. Biological properties of extracellular vesicles and their physiological functions. *J. Extracell. Vesicles* **2015**, *4*, 27066–27126.

[4] Chen, X.; Ba, Y.; Ma, L. J.; Cai, X.; Yin, Y.; Wang, K. H.; Guo, J. G.; Zhang, Y. J.; Chen, J. N.; Guo, X. et al. Characterization of microRNAs in serum: A novel class of biomarkers for diagnosis of cancer and other diseases. *Cell Res.* **2008**, *18*, 997–1006.

[5] Zaborowski, M. P.; Balaj, L.; Breakefield, X. O.; Lai, C. P. Extracellular vesicles: Composition, biological relevance, and methods of study. *Bioscience* **2015**, *65*, 783–797.

[6] Allen, T. M.; Cullis, P. R. Liposomal drug delivery systems: From concept to clinical applications. *Adv. Drug Deliv. Rev.* **2013**, *65*, 36–48.

[7] Riazifar, M.; Pone, E. J.; Lötvall, J.; Zhao, W. A. Stem cell extracellular vesicles: Extended messages of regeneration. *Ann. Rev. Pharmacol. Toxicol.* **2017**, *57*, 125–154.

[8] György, B.; Hung, M. E.; Breakefield, X. O.; Leonard, J. N. Therapeutic applications of extracellular vesicles: Clinical promise and open questions. *Ann. Rev. Pharmacol. Toxicol.* **2015**, *55*, 439–464.

[9] Chai, Z. L.; Hu, X. F.; Lu, W. Y. Cell membrane-coated nanoparticles for tumor-targeted drug delivery. *Sci. China Mater.* **2017**, *60*, 504–510.

[10] Calò, A.; Reguera, D.; Oncins, G.; Persuy, M. A.; Sanz, G.; Lobasso, S.; Corcelli, A.; Pajot-Augy, E.; Gomila, G. Force measurements on natural membrane nanovesicles reveal a composition-independent, high young's modulus. *Nanoscale* **2014**, *6*, 2275–2285.

[11] Chen, O.; Riedemann, L.; Etoc, F.; Herrmann, H.; Coppey, M.; Barch, M.; Farrar, C. T.; Zhao, J.; Bruns, O. T.; Wei, H. et al. Magneto-fluorescent core-shell supernanoparticles. *Nat. Commun.* **2014**, *5*, 5093-5101.

[12] Key, J.; Leary, J. F. Nanoparticles for multimodal *in vivo* imaging in nanomedicine. *Int. J. Nanomedicine* **2014**, *9*, 711–726.

[13] Chen, B.; Li, Y.; Zhang, X. Q.; Liu, F.; Liu, Y. L.; Ji, M.; Xiong, F.; Gu, N. An efficient synthesis of ferumoxytol induced by alternating-current magnetic field. *Mater. Lett.* **2016**, *170*, 93–96.

[14] Duan, L.; Yang, F.; He, W.; Song, L. N.; Qiu, F.; Xu, N.; Xu, L.; Zhang, Y.; Hua, Z. C.; Gu, N. A multi-gradient targeting drug delivery system based on RGD-$_L$-TRAIL-labeled magnetic microbubbles for cancer theranostics. *Adv. Funct. Mater.* **2016**, *26*, 8313–8324.

[15] Ma, X. X.; Tao, H. Q.; Yang, K.; Feng, L. Z.; Cheng, L.; Shi, X. Z.; Li, Y. G.; Guo, L.; Liu, Z. A functionalized graphene oxide-iron oxide nanocomposite for magnetically targeted drug delivery, photothermal therapy, and magnetic resonance imaging. *Nano Res.* **2012**, *5*, 199–212.

[16] Yigit, M. V.; Moore, A.; Medarova, Z. Magnetic nanoparticles for cancer diagnosis and therapy. *Pharm. Res.* **2012**, *29*, 1180–1188.

[17] Peer, D.; Karp, J. M.; Hong, S.; FaroKhzad, O. C.; Margalit, R.; Langer, R. Nanocarriers as an emerging platform for cancer therapy. *Nat. Nanotechnol.* **2007**, *2*, 751–760.

[18] Ding, Q.; Liu, D. F.; Guo, D. W.; Yang, F.; Pang, X. Y.; Che, R. C.; Zhou, N. Z.; Xie, J.; Sun, J. F.; Huang, Z. H. et al. Shape-controlled fabrication of magnetite silver hybrid nanoparticles with high performance magnetic hyperthermia. *Biomaterials* **2017**, *124*, 35–46.

[19] Wang, M.; Thanou, M. Targeting nanoparticles to cancer. *Pharmacol. Res.* **2010**, *62*, 90–99.

[20] Berman, S. M. C.; Walczak, P.; Bulte, J. W. M. Tracking stem cells using magnetic nanoparticles. *Wiley Interdiscip. Rev. Nanomed. Nanobiotechnol.* **2011**, *3*, 343–355.

[21] Li, L.; Jiang, W.; Luo, K.; Song, H. M.; Lan, F.; Wu, Y.; Gu, Z. W. Superparamagnetic iron oxide nanoparticles as mri contrast agents for non-invasive stem cell labeling and tracking. *Theranostics* **2013**, *3*, 595–615.

[22] Prashant, C.; Dipak, M.; Yang, C. T.; Chuang, K. H.; Jun, D.; Feng, S. S. Superparamagnetic iron oxide-loaded poly(lactic acid)-$_D$-α-tocopherol polyethylene glycol 1000 succinate copolymer nanoparticles as mri contrast agent. *Biomaterials* **2010**, *31*, 5588–5597.

[23] Kircher, M. F.; Gambhir, S. S.; Grimm, J. Noninvasive cell-tracking methods. *Nat. Rev. Clin. Oncol.* **2011**, *8*, 677–688.

[24] Behzadi, S.; Serpooshan, V.; Tao, W.; Hamaly, M. A.;

Alkawareek, M. Y.; Dreaden, E. C.; Brown, D.; Alkilany, A. M.; Farokhzad, O. C.; Mahmoudi, M. Cellular uptake of nanoparticles: Journey inside the cell. *Chem. Soc. Rev.* **2017**, *46*, 4218–4244.

[25] Gupta, A. K.; Gupta, M. Synthesis and surface engineering of iron oxide nanoparticles for biomedical applications. *Biomaterials* **2005**, *26*, 3995–4021.

[26] Mura, S.; Nicolas, J.; Couvreur, P. Stimuli-responsive nanocarriers for drug delivery. *Nat. Mater.* **2013**, *12*, 991–1003.

[27] Katagiri, K.; Imai, Y.; Koumoto, K.; Kaiden, T.; Kono, K.; Aoshima, S. Magnetoresponsive on-demand release of hybrid liposomes formed from Fe_3O_4 nanoparticles and thermosensitive block copolymers. *Small* **2011**, *7*, 1683–1689.

[28] Tassa, C.; Shaw, S. Y.; Weissleder, R. Dextran-coated iron oxide nanoparticles: A versatile platform for targeted molecular imaging, molecular diagnostics, and therapy. *Acc. Chem. Res.* **2011**, *44*, 842–852.

[29] Silva, A. K. A.; Luciani, N.; Gazeau, F.; Aubertin, K.; Bonneau, S.; Chauvierre, C.; Letourneur, D.; Wilhelm, C. Combining magnetic nanoparticles with cell derived microvesicles for drug loading and targeting. *Nanomed.-Nanotechnol. Biol. Med.* **2015**, *11*, 645–655.

[30] Tukmachev, D.; Lunov, O.; Zablotskii, V.; Dejneka, A.; Babic, M.; Syková, E.; Kubinová, Š. An effective strategy of magnetic stem cell delivery for spinal cord injury therapy. *Nanoscale* **2015**, *7*, 3954–3958.

[31] Penland, N.; Choi, E.; Perla, M.; Park, J.; Kim, D. H. Facile fabrication of tissue-engineered constructs using nanopatterned cell sheets and magnetic levitation. *Nanotechnology* **2017**, *28*, 075103–075111.

[32] Ho, V. H. B.; Müller, K. H.; Barcza, A.; Chen, R. J.; Slater, N. K. H. Generation and manipulation of magnetic multicellular spheroids. *Biomaterials* **2010**, *31*, 3095–3102.

[33] Ito, A.; Ino, K.; Hayashida, M.; Kobayashi, T.; Matsunuma, H.; Kagami, H.; Ueda, M.; Honda, H. Novel methodology for fabrication of tissue-engineered tubular constructs using magnetite nanoparticles and magnetic force. *Tissue Eng.* **2005**, *11*, 1553–1561.

[34] Whatley, B. R.; Li, X. W.; Zhang, N.; Wen, X. J. Magnetic-directed patterning of cell spheroids. *J. Biomed. Mater. Res. Part A* **2014**, *102*, 1537–1547.

[35] Boehm-Sturm, P.; Mengler, L.; Wecker, S.; Hoehn, M.; Kallur, T. *In vivo* tracking of human neural stem cells with ^{19}F magnetic resonance imaging. *PLoS One* **2011**, *6*, e29040–e29049.

[36] Daadi, M. M.; Li, Z. J.; Arac, A.; Grueter, B. A.; Sofilos, M.; Malenka, R. C.; Wu, J. C.; Steinberg, G. K. Molecular and magnetic resonance imaging of human embryonic stem cell-derived neural stem cell grafts in ischemic rat brain. *Mol. Ther.* **2009**, *17*, 1282–1291.

[37] Silva, A. K. A.; Wilhelm, C.; Kolosnjaj-Tabi, J.; Luciani, N.; Gazeau, F. Cellular transfer of magnetic nanoparticles via cell microvesicles: Impact on cell tracking by magnetic resonance imaging. *Pharm. Res.* **2012**, *29*, 1392–1403.

[38] Kumari, S.; Swetha, M. G.; Mayor, S. Endocytosis unplugged: Multiple ways to enter the cell. *Cell Res.* **2010**, *20*, 256–275.

[39] Mooren, O. L.; Galletta, B. J.; Cooper, J. A. Roles for actin assembly in endocytosis. *Annu. Rev. Biochem.* **2012**, *81*, 661–686.

[40] Porat-Shliom, N.; Milberg, O.; Masedunskas, A.; Weigert, R. Multiple roles for the actin cytoskeleton during regulated exocytosis. *Cell. Mol. Life Sci.* **2013**, *70*, 2099–2121.

[41] Lim, J. P.; Gleeson, P. A. Macropinocytosis: An endocytic pathway for internalising large gulps. *Immunol. Cell Biol.* **2011**, *89*, 836–843.

[42] de Vries, E.; Tscherne, D. M.; Wienholts, M. J.; Cobos-Jiménez, V.; Scholte, F.; García-Sastre, A.; Rottier, P. J. M.; de Haan, C. A. M. Dissection of the influenza a virus endocytic routes reveals macropinocytosis as an alternative entry pathway. *PLoS Pathog.* **2011**, *7*, e1001329–e1001348.

[43] Geiser, M. Update on macrophage clearance of inhaled micro- and nanoparticles. *J. Aerosol Med. Pulm. Drug Deliv.* **2010**, *23*, 207–217.

[44] Yameen, B.; Choi, W. I.; Vilos, C.; Swami, A.; Shi, J. J.; Farokhzad, O. C. Insight into nanoparticle cellular uptake and intracellular targeting. *J. Control. Release* **2014**, *190*, 485–499.

[45] Banerjee, A.; Berezhkovskii, A.; Nossal, R. Kinetics of cellular uptake of viruses and nanoparticles via clathrin-mediated endocytosis. *Phys. Biol.* **2016**, *13*, 016005–016018.

[46] Harush-Frenkel, O.; Altschuler, Y.; Benita, S. Nanoparticle-cell interactions: Drug delivery implications. *Crit. Rev. Ther. Drug Carr. Syst.* **2008**, *25*, 485–544.

[47] Pelkmans, L.; Kartenbeck, J.; Helenius, A. Caveolar endocytosis of simian virus 40 reveals a new two-step vesicular-transport pathway to the ER. *Nat. Cell Biol.* **2001**, *3*, 473–483.

[48] Rodríguez, N. E.; Gaur, U.; Wilson, M. E. Role of caveolae in *Leishmania chagasi* phagocytosis and intracellular survival in macrophages. *Cell Microbiol.* **2006**, *8*, 1106–1120.

[49] Li, W.; Chen, C. Y.; Ye, C.; Wei, T. T.; Zhao, Y. L.; Lao, F.; Chen, Z.; Meng, H.; Gao, Y. X.; Yuan, H. et al. The translocation of fullerenic nanoparticles into lysosome via the pathway of clathrin-mediated endocytosis. *Nanotechnology* **2008**, *19*, 145102.

[50] Bryant, L. H.; Kim, S. J.; Hobson, M.; Milo, B.; Kovacs, Z. I.; Jikaria, N.; Lewis, B. K.; Aronova, M. A.; Sousa, A. A.; Zhang, G. F. et al. Physicochemical characterization of ferumoxytol, heparin and protamine nanocomplexes for improved

magnetic labeling of stem cells. *Nanomed.-Nanotechnol. Biol. Med.* **2017**, *13*, 503–513.

[51] Du, B. J.; Liu, J. H.; Ding, G. Y.; Han, X.; Li, D.; Wang, E. K.; Wang, J. Positively charged graphene/Fe_3O_4/polyethylenimine with enhanced drug loading and cellular uptake for magnetic resonance imaging and magnet-responsive cancer therapy. *Nano Res.* **2017**, *10*, 2280–2295.

[52] Candeloro, P.; Tirinato, L.; Malara, N.; Fregola, A.; Casals, E.; Puntes, V.; Perozziello, G.; Gentile, F.; Coluccio, M. L.; Das, G. et al. Nanoparticle microinjection and raman spectroscopy as tools for nanotoxicology studies. *Analyst* **2011**, *136*, 4402–4408.

[53] Walczak, P.; Ruiz-Cabello, J.; Kedziorek, D. A.; Gilad, A. A.; Lin, S. P.; Barnett, B.; Qin, L.; Levitsky, H.; Bulte, J. W. M. Magnetoelectroporation: Improved labeling of neural stem cells and leukocytes for cellular magnetic resonance imaging using a single FDA-approved agent. *Nanomed.-Nanotechnol. Biol. Med.* **2006**, *2*, 89–94.

[54] Yang, F.; Li, M. X.; Cui, H. T.; Wang, T. T.; Chen, Z. W.; Song, L. N.; Gu, Z. X.; Zhang, Y.; Gu, N. Altering the response of intracellular reactive oxygen to magnetic nanoparticles using ultrasound and microbubbles. *Sci. China. Mater.* **2015**, *58*, 467–480.

[55] Lee, C. H.; Chen, C. B.; Chung, T. H.; Lin, Y. S.; Lee, W. C. Cellular uptake of protein-bound magnetic nanoparticles in pulsed magnetic field. *J. Nanosci. Nanotechnol.* **2010**, *10*, 7965–7970.

[56] Ye, D. W; Wang, Q. W; Zhang, W. G; Sun, J. F; Gu, N. Recent progress in magnetic labeling for stem cell, *Chin. Sci. Bull.* **2017**, *62*, 2301–2311.

[57] Cui, Y. N.; Xu, Q. X.; Chow, P. K. H.; Wang, D. P.; Wang, C. H. Transferrin-conjugated magnetic silica plga nanoparticles loaded with doxorubicin and paclitaxel for brain glioma treatment. *Biomaterials* **2013**, *34*, 8511–8520.

[58] Song, M.; Moon, W. K.; Kim, Y.; Lim, D.; Song, I. C.; Yoon, B. W. Labeling efficacy of superparamagnetic iron oxide nanoparticles to human neural stem cells: Comparison of ferumoxides, monocrystalline iron oxide, cross-linked iron oxide (CLIO)-NH_2 and tat-CLIO. *Korean J. Radiol.* **2007**, *8*, 365–371.

[59] Wang, C. H.; Qiao, L.; Zhang, Q.; Yan, H. S.; Liu, K. L. Enhanced cell uptake of superparamagnetic iron oxide nanoparticles through direct chemisorption of FITC-tat-PEG_{600}-b-poly(glycerol monoacrylate). *Int. J. Pharm.* **2012**, *430*, 372–380.

[60] Andreas, K.; Georgieva, R.; Ladwig, M.; Mueller, S.; Notter, M.; Sittinger, M.; Ringe, J. Highly efficient magnetic stem cell labeling with citrate-coated superparamagnetic iron oxide nanoparticles for MRI tracking. *Biomaterials* **2012**, *33*, 4515–4525.

[61] Frank, J. A.; Miller, B. R.; Arbab, A. S.; Zywicke, H. A.; Jordan, E. K.; Lewis, B. K.; Bryant, L. H. Jr; Bulte, J. W. M. Clinically applicable labeling of mammalian and stem cells by combining superparamagnetic iron oxides and transfection agents. *Radiology* **2003**, *228*, 480–487.

[62] Min, K. A.; Shin, M. C.; Yu, F. Q.; Yang, M. Z.; David, A. E.; Yang, V. C.; Rosania, G. R. Pulsed magnetic field improves the transport of iron oxide nanoparticles through cell barriers. *ACS Nano* **2013**, *7*, 2161–2171.

[63] Xie, D. H.; Qiu, B. S.; Walczak, P.; Li, X. B.; Ruiz-Cabello, J.; Minoshima, S.; Bulte, J. W. M.; Yang, X. M. Optimization of magnetosonoporation for stem cell labeling. *NMR Biomed.* **2010**, *23*, 480–484.

[64] Guduru, R.; Liang, P.; Runowicz, C.; Nair, M.; Atluri, V.; Khizroev, S. Magneto-electric nanoparticles to enable field-controlled high-specificity drug delivery to eradicate ovarian cancer cells. *Sci. Rep.* **2013**, *3*, 2953.

[65] Vats, N.; Wilhelm, C.; Rautou, P. E.; Poirier-Quinot, M.; Péchoux, C.; Devue, C.; Boulanger, C. M.; Gazeau, F. Magnetic tagging of cell-derived microparticles: New prospects for imaging and manipulation of these mediators of biological information. *Nanomedicine* **2010**, *5*, 727–738.

[66] Klein, S.; Sommer, A.; Distel, L. V. R.; Neuhuber, W.; Kryschi, C. Superparamagnetic iron oxide nanoparticles as radiosensitizer via enhanced reactive oxygen species formation. *Biochem. Biophys. Res. Common.* **2012**, *425*, 393–397.

[67] Chen, Z. W.; Yin, J. J.; Zhou, Y. T.; Zhang, Y.; Song, L.; Song, M. J.; Hu, S. L.; Gu, N. Dual enzyme-like activities of iron oxide nanoparticles and their implication for diminishing cytotoxicity. *ACS Nano* **2012**, *6*, 4001–4012.

[68] Geng, Y.; Dalhaimer, P.; Cai, S. S.; Tsai, R.; Tewari, M.; Minko, T.; Discher, D. E. Shape effects of filaments versus spherical particles in flow and drug delivery. *Nat. Nanotechnol.* **2007**, *2*, 249–255.

[69] Park, J. H.; von Maltzahn, G.; Zhang, L. L.; Schwartz, M. P.; Ruoslahti, E.; Bhatia, S. N.; Sailor, M. J. Magnetic iron oxide nanoworms for tumor targeting and imaging. *Adv. Mater.* **2008**, *20*, 1630–1635.

[70] Li, X.; Bao, M. M.; Weng, Y. Y.; Yang, K.; Zhang, W. D.; Chen, G. J. Glycopolymer-coated iron oxide nanoparticles: Shape-controlled synthesis and cellular uptake. *J. Mat. Chem. B* **2014**, *2*, 5569–5575.

[71] Ulrich, S.; Hirsch, C.; Diener, L.; Wick, P.; Rossi, R. M.; Bannwarth, M. B.; Boesel, L. F. Preparation of ellipsoid-shaped supraparticles with modular compositions and investigation of shape-dependent cell-uptake. *RSC Adv.* **2016**, *6*, 89028–89039.

[72] Liu, Z.; Cai, W. B.; He, L. N.; Nakayama, N.; Chen, K.; Sun, X. M.; Chen, X. Y.; Dai, H. J. *In vivo* biodistribution and

highly efficient tumour targeting of carbon nanotubes in mice. *Nat. Nanotechnol*. **2007**, *2*, 47–52.

[73] Sherwood, J.; Lovas, K.; Rich, M.; Yin, Q.; Lackey, K.; Bolding, M. S.; Bao, Y. Shape-dependent cellular behaviors and relaxivity of iron oxide-based T_1 MRI contrast agents. *Nanoscale* **2016**, *8*, 17506–17515.

[74] Sun, Z. Z.; Worden, M.; Wroczynskyj, Y.; Manna, P. K.; Thliveris, J. A.; van Lierop, J.; Hegmann, T.; Miller, D. W. Differential internalization of brick shaped iron oxide nanoparticles by endothelial cells. *J. Mat. Chem. B* **2016**, *4*, 5913–5920.

[75] Yu, S. S.; Lau, C. M.; Thomas, S. N.; Jerome, W. G.; Maron, D. J.; Dickerson, J. H.; Hubbell, J. A.; Giorgio, T. D. Size- and charge-dependent non-specific uptake of pegylated nanoparticles by macrophages. *Int. J. Nanomedicine* **2012**, *7*, 799–813.

[76] Trekker, J.; Leten, C.; Struys, T.; Lazenka, V. V.; Argibay, B.; Micholt, L.; Lambrichts, I.; Van Roy, W.; Lagae, L.; Himmelreich, U. Sensitive *in vivo* cell detection using size-optimized superparamagnetic nanoparticles. *Biomaterials* **2014**, *35*, 1627–1635.

[77] Jun, Y. W.; Huh, Y. M.; Choi, J. S.; Lee, J. H.; Song, H. T.; Kim, S.; Yoon, S.; Kim, K. S.; Shin, J. S.; Suh, J. S. et al. Nanoscale size effect of magnetic nanocrystals and their utilization for cancer diagnosis via magnetic resonance imaging. *J. Am. Chem. Soc.* **2005**, *127*, 5732–5733.

[78] Jun, Y. W.; Lee, J. H.; Cheon, J. Chemical design of nanoparticle probes for high-performance magnetic resonance imaging. *Angew. Chem., Int. Ed.* **2008**, *47*, 5122–5135.

[79] Tanimoto, A.; Kuribayashi, S. Application of superparamagnetic iron oxide to imaging of hepatocellular carcinoma. *Eur. J. Radiol*. **2006**, *58*, 200–216.

[80] Huang, J.; Bu, L. H.; Xie, J.; Chen, K.; Cheng, Z.; Li, X. G.; Chen, X. Y. Effects of nanoparticle size on cellular uptake and liver MRI with polyvinylpyrrolidone-coated iron oxide nanoparticles. *ACS Nano* **2010**, *4*, 7151–7160.

[81] He, C. B.; Hu, Y. P.; Yin, L. C.; Tang, C.; Yin, C. H. Effects of particle size and surface charge on cellular uptake and biodistribution of polymeric nanoparticles. *Biomaterials* **2010**, *31*, 3657–3666.

[82] Mendes, R. G.; Koch, B.; Bachmatiuk, A.; El-Gendy, A. A.; Krupskaya, Y.; Springer, A.; Klingeler, R.; Schmidt, O.; Buchner, B.; Sanchez, S. et al. Synthesis and toxicity characterization of carbon coated iron oxide nanoparticles with highly defined size distributions. *Biochim. Biophys. Acta-Gen. Subj*. **2014**, *1840*, 160–169.

[83] Shang, L.; Nienhaus, K.; Nienhaus, G. U. Engineered nanoparticles interacting with cells: Size matters. *J. Nanobiotechnol.* **2014**, *12*, 5–16.

[84] Sun, R.; Dittrich, J.; Le-Huu, M.; Mueller, M. M.; Bedke, J.; Kartenbeck, J.; Lehmann, W. D.; Krueger, R.; Bock, M.; Huss, R. et al. Physical and biological characterization of superparamagnetic iron oxide- and ultrasmall superparamagnetic iron oxide-labeled cells - a comparison. *Invest. Radiol.* **2005**, *40*, 504–513.

[85] Jo, J.; Aoki, I.; Tabata, Y. Design of iron oxide nanoparticles with different sizes and surface charges for simple and efficient labeling of mesenchymal stem cells. *J. Control. Release* **2010**, *142*, 465–473.

[86] Yuan, H. Y.; Li, J.; Bao, G.; Zhang, S. L. Variable nanoparticle-cell adhesion strength regulates cellular uptake. *Phys. Rev. Lett.* **2010**, *105*, 138101–138105.

[87] Zhang, S. L.; Gao, H. J.; Bao, G. Physical principles of nanoparticle cellular endocytosis. *ACS Nano* **2015**, *9*, 8655–8671.

[88] Deserno, M.; Bickel, T. Wrapping of a spherical colloid by a fluid membrane. *Europhys. Lett.* **2003**, *62*, 767–774.

[89] Lin, X. B.; Li, Y.; Gu, N. Nanoparticle's size effect on its translocation across a lipid bilayer: A molecular dynamics simulation. *J. Comput. Theor. Nanosci.* **2010**, *7*, 269–276.

[90] Gal, N.; Lassenberger, A.; Herrero-Nogareda, L.; Scheberl, A.; Charwat, V.; Kasper, C.; Reimhult, E. Interaction of size-tailored pegylated iron oxide nanoparticles with lipid membranes and cells. *ACS Biomater. Sci. Eng.* **2017**, *3*, 249–259.

[91] Hu, Z. Y.; Zhang, H. Y.; Zhang, Y.; Wu, R. A.; Zou, H. F. Nanoparticle size matters in the formation of plasma protein coronas on Fe_3O_4 nanoparticles. *Colloid Surf. B-Biointerfaces* **2014**, *121*, 354–361.

[92] Mahmoudi, M.; Sheibani, S.; Milani, A. S.; Rezaee, F.; Gauberti, M.; Dinarvand, R.; Vali, H. Crucial role of the protein corona for the specific targeting of nanoparticles. *Nanomedicine* **2015**, *10*, 215–226.

[93] Punnakitikashem, P.; Chang, S. H.; Huang, C. W.; Liu, J. P.; Hao, Y. W. Design and fabrication of non-superparamagnetic high moment magnetic nanoparticles for bioapplications. *J. Nanopart. Res.* **2010**, *12*, 1101–1106.

[94] Assa, F.; Jafarizadeh-Malmiri, H.; Ajamein, H.; Anarjan, N.; Vaghari, H.; Sayyar, Z.; Berenjian, A. A biotechnological perspective on the application of iron oxide nanoparticles. *Nano Res.* **2016**, *9*, 2203–2225.

[95] Hamley, I. W. Nanotechnology with soft materials. *Angew. Chem., Int. Ed.* **2003**, *42*, 1692–1712.

[96] Fayol, D.; Luciani, N.; Lartigue, L.; Gazeau, F.; Wilhelm, C. Managing magnetic nanoparticle aggregation and cellular uptake: A precondition for efficient stem-cell differentiation and mri tracking. *Adv. Healthc. Mater.* **2013**, *2*, 313–325.

[97] Safi, M.; Sarrouj, H.; Sandre, O.; Mignet, N.; Berret, J. F. Interactions between sub-10-nm iron and cerium oxide

nanoparticles and 3T3 fibroblasts: The role of the coating and aggregation state. *Nanotechnology* **2010**, *21*, 145103–145113.

[98] Bae, J. E.; Huh, M. I.; Ryu, B. K.; Do, J. Y.; Jin, S. U.; Moon, M. J.; Jung, J. C.; Chang, Y.; Kim, E.; Chi, S. G. et al. The effect of static magnetic fields on the aggregation and cytotoxicity of magnetic nanoparticles. *Biomaterials* **2011**, *32*, 9401–9414.

[99] Herve, K.; Douziech-Eyrolles, L.; Munnier, E.; Cohen-Jonathan, S.; Soucé, M.; Marchais, H.; Limelette, P.; Warmont, F.; Saboungi, M. L.; Dubois, P. et al. The development of stable aqueous suspensions of pegylated spions for biomedical applications. *Nanotechnology* **2008**, *19*, 465608–465615.

[100] Gillich, T.; Acikgoz, C.; Isa, L.; Schluter, A. D.; Spencer, N. D.; Textor, M. Peg-stabilized core-shell nanoparticles: Impact of linear versus dendritic polymer shell architecture on colloidal properties and the reversibility of temperature-induced aggregation. *ACS Nano* **2013**, *7*, 316–329.

[101] Mornet, S.; Portier, J.; Duguet, E. A method for synthesis and functionalization of ultrasmall superparamagnetic covalent carriers based on maghemite and dextran. *J. Magn. Magn. Mater.* **2005**, *293*, 127–134.

[102] Duan, H. W.; Kuang, M.; Wang, X. X.; Wang, Y. A.; Mao, H.; Nie, S. M. Reexamining the effects of particle size and surface chemistry on the magnetic properties of iron oxide nanocrystals: New insights into spin disorder and proton relaxivity. *J. Phys. Chem. C* **2008**, *112*, 8127–8131.

[103] Zhao, X. Q.; Shang, T.; Zhang, X. D.; Ye, T.; Wang, D. J.; Rei, L. Passage of magnetic tat-conjugated Fe_3O_4@SiO_2 nanoparticles across *in vitro* blood-brain barrier. *Nanoscale Res. Lett.* **2016**, *11*, 451–463.

[104] Zhang, J.; Chen, Y. C.; Li, X.; Liang, X. L.; Luo, X. J. The influence of different long-circulating materials on the pharmacokinetics of liposomal vincristine sulfate. *Int. J. Nanomed.* **2016**, *11*, 4187–4197.

[105] Mosqueira, V. C. F.; Legrand, P.; Morgat, J. L.; Vert, M.; Mysiakine, E.; Gref, R.; Devissaguet, J. P.; Barratt, G. Biodistribution of long-circulating PEG-grafted nanocapsules in mice: Effects of peg chain length and density. *Pharm. Res.* **2001**, *18*, 1411–1419.

[106] Mohamed, S. A.; Al-Harbi, M. H.; Almulaiky, Y. Q.; Ibrahim, I. H.; El-Shishtawy, R. M. Immobilization of horseradish peroxidase on Fe_3O_4 magnetic nanoparticles. *Electron. J. Biotechnol.* **2017**, *27*, 84–90.

[107] Ahn, J.; Moon, D. S.; Lee, J. K. Arsonic acid as a robust anchor group for the surface modification of Fe_3O_4. *Langmuir* **2013**, *29*, 14912–14918.

[108] Park, J.; Kadasala, N. R.; Abouelmagd, S. A.; Castanares, M. A.; Collins, D. S.; Wei, A.; Yeo, Y. Polymer-iron oxide composite nanoparticles for epr-independent drug delivery. *Biomaterials* **2016**, *101*, 285–295.

[109] Dowaidar, M.; Abdelhamid, H. N.; Hällbrink, M.; Freimann, K.; Kurrikoff, K.; Zou, X. D.; Langel, Ü. Magnetic nanoparticle assisted self-assembly of cell penetrating peptides-oligonucleotides complexes for gene delivery. *Sci. Rep.* **2017**, *7*, 9159–9170.

[110] Gao, L. P.; Yu, J.; Liu, Y.; Zhou, J. E.; Sun, L.; Wang, J.; Zhu, J. Z.; Peng, H.; Lu, W. Y.; Yu, L. et al. Tumor-penetrating peptide conjugated and doxorubicin loaded T_1-T_2 dual mode mri contrast agents nanoparticles for tumor theranostics. *Theranostics* **2018**, *8*, 92–108.

[111] Li, X. M.; Ding, L. Y.; Xu, Y. L.; Wang, Y. L.; Ping, Q. N. Targeted delivery of doxorubicin using stealth liposomes modified with transferrin. *Int. J. Pharm.* **2009**, *373*, 116–123.

[112] Ståhl, S.; Gräslund, T.; Karlström, A. E.; Frejd, F. Y.; Nygren, P. Ä.; Löfblom, J. Affibody molecules in biotechnological and medical applications. *Trends Biotechnol.* **2017**, *35*, 691–712.

[113] Chai, Z. L.; Hu, X. F.; Wei, X. L.; Zhan, C. Y.; Lu, L. W.; Jiang, K.; Su, B. X.; Ruan, H. T.; Ran, D. N.; Fang, R. H. et al. A facile approach to functionalizing cell membrane-coated nanoparticles with neurotoxin-derived peptide for brain-targeted drug delivery. *J. Control. Release* **2017**, *264*, 102–111.

[114] Osaka, T.; Nakanishi, T.; Shanmugam, S.; Takahama, S.; Zhang, H. Effect of surface charge of magnetite nanoparticles on their internalization into breast cancer and umbilical vein endothelial cells. *Colloid Surf. B-Biointerfaces* **2009**, *71*, 325–330.

[115] Wang, X. Q.; Zhang, H. R.; Jing, H. J.; Cui, L. Q. Highly efficient labeling of human lung cancer cells using cationic poly-L-lysine-assisted magnetic iron oxide nanoparticles. *Nano-Micro Lett.* **2015**, *7*, 374–384.

[116] Bull, E.; Madani, S. Y.; Sheth, R.; Seifalian, A.; Green, M.; Seifalian, A. M. Stem cell tracking using iron oxide nanoparticles. *Int. J. Nanomed.* **2014**, *9*, 1641–1653.

[117] Santhosh, P. B.; Velikonja, A.; Perutkova, Š.; Gongadze, E.; Kulkarni, M.; Genova, J.; Eleršič, K.; Iglič, A.; Kralj-Iglič, V.; Ulrih, N. P. Influence of nanoparticle-membrane electrostatic interactions on membrane fluidity and bending elasticity. *Chem. Phys. Lipids* **2014**, *178*, 52–62.

[118] Lin, J. Q.; Zhang, H. W.; Chen, Z.; Zheng, Y. G. Penetration of lipid membranes by gold nanoparticles: Insights into cellular uptake, cytotoxicity, and their relationship. *ACS Nano* **2010**, *4*, 5421–5429.

[119] Nangia, S.; Sureshkumar, R. Effects of nanoparticle charge and shape anisotropy on translocation through cell membranes. *Langmuir* **2012**, *28*, 17666–17671.

[120] Li, S.; Malmstadt, N. Deformation and poration of lipid bilayer membranes by cationic nanoparticles. *Soft Matter* **2013**, *9*, 4969–4976.

[121] Deen, W. M.; Bohrer, M. P.; Epstein, N. B. Effects of molecular size and configuration on diffusion in microporous membranes. *AIChE J.* **1981**, *27*, 952–959.

[122] Hong, S. P.; Leroueil, P. R.; Janus, E. K.; Peters, J. L.; Kober, M. M.; Islam, M. T.; Orr, B. G.; Baker, J. R.; Holl, M. M. B. Interaction of polycationic polymers with supported lipid bilayers and cells: Nanoscale hole formation and enhanced membrane permeability. *Bioconjugate Chem.* **2006**, *17*, 728–734.

[123] Wang, T. T.; Bai, J.; Jiang, X.; Nienhaus, G. U. Cellular uptake of nanoparticles by membrane penetration: A study combining confocal microscopy with ftir spectroelectrochemistry. *ACS Nano* **2012**, *6*, 1251–1259.

[124] Han, X.; Deng, Z. C.; Yang, Z.; Wang, Y. L.; Zhu, H. H.; Chen, B. D.; Cui, Z.; Ewing, R. C.; Shi, D. L. Biomarkerless targeting and photothermal cancer cell killing by surface-electrically-charged superparamagnetic Fe_3O_4 composite nanoparticles. *Nanoscale* **2017**, *9*, 1457–1465.

[125] Pu, L.; Xu, J. B.; Sun, Y. M.; Fang, Z.; Chan-Park, M. B.; Duan, H. W. Cationic polycarbonate-grafted superparamagnetic nanoparticles with synergistic dual-modality antimicrobial activity. *Biomater. Sci.* **2016**, *4*, 871–879.

[126] Sakulkhu, U.; Mahmoudi, M.; Maurizi, L.; Coullerez, G.; Hofmann-Amtenbrink, M.; Vries, M.; Motazacker, M.; Rezaee, F.; Hofmann, H. Significance of surface charge and shell material of superparamagnetic iron oxide nanoparticle (SPION) based core/shell nanoparticles on the composition of the protein corona. *Biomater. Sci.* **2015**, *3*, 265–278.

[127] Fleischer, C. C.; Payne, C. K. Nanoparticle-cell interactions: Molecular structure of the protein corona and cellular outcomes. *Acc. Chem. Res.* **2014**, *47*, 2651–2659.

[128] Carter, D. C.; Ho, J. X. Structure of serum-albumin. *Adv. Protein Chem*. **1994**, *45*, 153–203.

[129] Mu, Q. X.; Li, Z. W.; Li, X.; Mishra, S. R.; Zhang, B.; Si, Z. K.; Yang, L.; Jiang, W.; Yan, B. Characterization of protein clusters of diverse magnetic nanoparticles and their dynamic interactions with human cells. *J. Phys. Chem. C* **2009**, *113*, 5390–5395.

[130] Serda, R. E.; Blanco, E.; Mack, A.; Stafford, S. J.; Amra, S.; Li, Q. P.; van de Ven, A.; Tanaka, T.; Torchilin, V. P.; Wiktorowicz, J. E. et al. Proteomic analysis of serum opsonins impacting biodistribution and cellular association of porous silicon microparticles. *Mol. Imaging* **2011**, *10*, 43–55.

[131] McConnell, K. I.; Shamsudeen, S.; Meraz, I. M.; Mahadevan, T. S.; Ziemys, A.; Rees, P.; Summers, H. D.; Serda, R. E. Reduced cationic nanoparticle cytotoxicity based on serum masking of surface potential. *J. Biomed. Nanotechnol*. **2016**, *12*, 154–164.

[132] Babič, M.; Horák, D.; Trchová, M.; Jendelová, P.; Glogarová, K.; Lesný, P.; Herynek, V.; Hájek, M.; Syková, E. Poly($_L$-lysine)-modified iron oxide nanoparticles for stem cell labeling. *Bioconjugate Chem*. **2008**, *19*, 740–750.

[133] Kokkinopoulou, M.; Simon, J.; Landfester, K.; Mailänder, V.; Lieberwirth, I. Visualization of the protein corona: Towards a biomolecular understanding of nanoparticle-cell-interactions. *Nanoscale* **2017**, *9*, 8858–8870.

[134] Gref, R.; Lück, M.; Quellec, P.; Marchand, M.; Dellacherie, E.; Harnisch, S.; Blunk, T.; Müller, R. H. 'Stealth' corona-core nanoparticles surface modified by polyethylene glycol (PEG): Influences of the corona (PEG chain length and surface density) and of the core composition on phagocytic uptake and plasma protein adsorption. *Colloid Surf. B-Biointerfaces* **2000**, *18*, 301–313.

[135] Ritz, S.; Schöttler, S.; Kotman, N.; Baier, G.; Musyanovych, A.; Kuharev, J.; Landfester, K.; Schild, H.; Jahn, O.; Tenzer, S. et al. Protein corona of nanoparticles: Distinct proteins regulate the cellular uptake. *Biomacromolecules* **2015**, *16*, 1311–1321.

[136] Rogers, W. J.; Basu, P. Factors regulating macrophage endocytosis of nanoparticles: Implications for targeted magnetic resonance plaque imaging. *Atherosclerosis* **2005**, *178*, 67–73.

[137] Ayala, V.; Herrera, A. P.; Latorre-Esteves, M.; Torres-Lugo, M.; Rinaldi, C. Effect of surface charge on the colloidal stability and *in vitro* uptake of carboxymethyl dextran-coated iron oxide nanoparticles. *J. Nanopart. Res*. **2013**, *15*, 2180–2186.

[138] Ge, Y. Q.; Zhang, Y.; Xia, J. G.; Ma, M.; He, S. Y.; Nie, F.; Gu, N. Effect of surface charge and agglomerate degree of magnetic iron oxide nanoparticles on kb cellular uptake *in vitro*. *Colloid Surf. B-Biointerfaces* **2009**, *73*, 294–301.

[139] Jahn, M. R.; Nawroth, T.; Fütterer, S.; Wolfrum, U.; Kolb, U.; Langguth, P. Iron oxide/hydroxide nanoparticles with negatively charged shells show increased uptake in CaCO-2 cells. *Mol. Pharmaceutics* **2012**, *9*, 1628–1637.

[140] Xu, Y. L.; Sherwood, J. A.; Lackey, K. H.; Qin, Y.; Bao, Y. P. The responses of immune cells to iron oxide nanoparticles. *J. Appl. Toxicol.* **2016**, *36*, 543–553.

[141] Srivastava, I.; Misra, S. K.; Ostadhossein, F.; Daza, E.; Singh, J.; Pan, D. Surface chemistry of carbon nanoparticles functionally select their uptake in various stages of cancer cells. *Nano Res.* **2017**, *10*, 3269–3284.

[142] Yang, Y.; Wang, Q. Q.; Song, L. N.; Liu, X.; Zhao, P.; Zhang, F. M.; Gu, N.; Sun, J. F. Uptake of magnetic nanoparticles for adipose-derived stem cells with multiple passage numbers. *Sci. China. Mater.* **2017**, *60*, 892–902.

[143] Wahajuddin; Arora, S. Superparamagnetic iron oxide nanoparticles: Magnetic nanoplatforms as drug carriers. *Int. J. Nanomedicine* **2012**, *7*, 3445–3471.

[144] Lu, Y. C.; Chang, F. Y.; Tu, S. J.; Chen, J. P.; Ma, Y. H. Cellular uptake of magnetite nanoparticles enhanced by NdFeB magnets in staggered arrangement. *J. Magn. Magn.*

Mater. **2017**, *427*, 71–80.

[145] Widder, K. J.; Senyei, A. E.; Scarpelli, D. G. Magnetic microspheres–A model system for site specific drug delivery *in vivo*. *Exp. Biol. Med.* **1978**, *158*, 141–146.

[146] Lamkowsky, M. C.; Geppert, M.; Schmidt, M. M.; Dringen, R. Magnetic field-induced acceleration of the accumulation of magnetic iron oxide nanoparticles by cultured brain astrocytes. *J. Biomed. Mater. Res. Part A* **2012**, *100A*, 323–334.

[147] MacDonald, C.; Barbee, K.; Polyak, B. Force dependent internalization of magnetic nanoparticles results in highly loaded endothelial cells for use as potential therapy delivery vectors. *Pharm. Res.* **2012**, *29*, 1270–1281.

[148] Barnes, A. L.; Wassel, R. A.; Mondalek, F.; Chen, K. J.; Dormer, K. J.; Kopke, R. D. Magnetic characterization of superparamagnetic nanoparticles pulled through model membranes. *BioMagnetic Res. Technol.* **2007**, *5*, 1.

[149] Chaudhary, S.; Smith, C. A.; del Pino, P.; de la Fuente, J. M.; Mullin, M.; Hursthouse, A.; Stirling, D.; Berry, C. C. Elucidating the function of penetratin and a static magnetic field in cellular uptake of magnetic nanoparticles. *Pharmaceuticals* **2013**, *6*, 204–222.

[150] Towhidi, L.; Firoozabadi, S. M. P.; Mozdarani, H.; Miklavcic, D. Lucifer yellow uptake by CHO cells exposed to magnetic and electric pulses. *Radiol. Oncol.* **2012**, *46*, 119–125.

[151] Chen, C. B.; Chen, J. Y.; Lee, W. C. Fast transfection of mammalian cells using superparamagnetic nanoparticles under strong magnetic field. *J. Nanosci. Nanotechnol.* **2009**, *9*, 2651–2659.

[152] Antov, Y.; Barbul, A.; Mantsur, H.; Korenstein, R. Electroendocytosis: Exposure of cells to pulsed low electric fields enhances adsorption and uptake of macromolecules. *Biophys. J.* **2005**, *88*, 2206–2223.

[153] Mahrour, N.; Pologea-Moraru, R.; Moisescu, M. G.; Orlowski, S.; Levêque, P.; Mir, L. M. *In vitro* increase of the fluid-phase endocytosis induced by pulsed radiofrequency electromagnetic fields: Importance of the electric field component. *Biochim. Biophys. Acta-Biomembr.* **2005**, *1668*, 126–137.

[154] Novickij, V.; Grainys, A.; Novickij, J.; Markovskaja, S. Irreversible magnetoporation of micro-organisms in high pulsed magnetic fields. *IET Nanobiotechnol.* **2014**, *8*, 157–162.

[155] Novickij, V.; Grainys, A.; Švediene, J.; Markovskaja, S.; Paškevičius, A.; Novickij, J. Microsecond pulsed magnetic field improves efficacy of antifungal agents on pathogenic microorganisms. *Bioelectromagnetics* **2014**, *35*, 347–353.

[156] Zhang, Z. H.; Lin, X. B.; Gu, N. Effects of temperature and peg grafting density on the translocation of pegylated nanoparticles across asymmetric lipid membrane. *Colloid Surf. B-Biointerfaces* **2017**, *160*, 92–100.

[157] Mailänder, V.; Lorenz, M. R.; Holzapfel, V.; Musyanovych, A.; Fuchs, K.; Wiesneth, M.; Walther, P.; Landfester, K.; Schrezenmeier, H. Carboxylated superparamagnetic iron oxide particles label cells intracellularly without transfection agents. *Mol. Imaging Biol.* **2008**, *10*, 138–146.

[158] Gal, N.; Massalha, S.; Samuelly-Nafta, O.; Weihs, D. Effects of particle uptake, encapsulation, and localization in cancer cells on intracellular applications. *Med. Eng. Phys.* **2015**, *37*, 478–483.

[159] Perevedentseva, E.; Hong, S. F.; Huang, K. J.; Chiang, I. T.; Lee, C. Y.; Tseng, Y. T.; Cheng, C. L. Nanodiamond internalization in cells and the cell uptake mechanism. *J. Nanopart. Res.* **2013**, *15*, 1834–1846.

[160] Srinivasan, A. R.; Lakshmikuttyamma, A.; Shoyele, S. A. Investigation of the stability and cellular uptake of self-associated monoclonal antibody (MAb) nanoparticles by non-small lung cancer cells. *Mol. Pharmaceutics* **2013**, *10*, 3275–3284.

[161] Rappoport, J. Z.; Simon, S. M. Endocytic trafficking of activated egfr is AP-2 dependent and occurs through preformed clathrin spots. *J. Cell Sci.* **2009**, *122*, 1301–1305.

[162] Kawauchi, T. Cell adhesion and its endocytic regulation in cell migration during neural development and cancer metastasis. *Int. J. Mol. Sci.* **2012**, *13*, 4564–4590.

[163] Bitsikas, V.; Corrêa, I. R. Jr.; Nichols, B. J. Clathrin-independent pathways do not contribute significantly to endocytic flux. *eLife* **2014**, *3*, e03970–e03996.

[164] Yalçin, S.; Özluer, Ö.; Gündüz, U. Nanoparticle-based drug delivery in cancer: The role of cell membrane structures. *Ther. Deliv.* **2016**, *7*, 773–781.

[165] Sahay, G.; Kim, J. O.; Kabanov, A. V.; Bronich, T. K. The exploitation of differential endocytic pathways in normal and tumor cells in the selective targeting of nanoparticulate chemotherapeutic agents. *Biomaterials* **2010**, *31*, 923–933.

[166] Sigismund, S.; Confalonieri, S.; Ciliberto, A.; Polo, S.; Scita, G.; Di Fiore, P. P. Endocytosis and signaling: Cell logistics shape the eukaryotic cell plan. *Physiol. Rev.* **2012**, *92*, 273–366.

[167] Zink, D.; Fischer, A. H.; Nickerson, J. A. Nuclear structure in cancer cells. *Nat. Rev. Cancer* **2004**, *4*, 677–687.

[168] Lekka, M.; Pogoda, K.; Gostek, J.; Klymenko, O.; Prauzner-Bechcicki, S.; Wiltowska-Zuber, J.; Jaczewska, J.; Lekki, J.; Stachura, Z. Cancer cell recognition–Mechanical phenotype. *Micron* **2012**, *43*, 1259–1266.

[169] Alibert, C.; Goud, B.; Manneville, J. B. Are cancer cells really softer than normal cells? *Biol. Cell* **2017**, *109*, 167–189.

[170] Hall, A. The cytoskeleton and cancer. *Cancer Metastasis Rev.* **2009**, *28*, 5–14.

[171] Grady, M. E.; Composto, R. J.; Eckmann, D. M. Cell elasticity with altered cytoskeletal architectures across multiple cell types. *J. Mech. Behav. Biomed.* **2016**, *61*, 197–207.

[172] Yilmaz, M.; Christofori, G. EMT, the cytoskeleton, and cancer cell invasion. *Cancer Metastasis Rev.* **2009**, *28*, 15–33.

[173] Elkhatib, N.; Bresteau, E.; Baschieri, F.; Rioja, A. L.; van Niel, G.; Vassilopoulos, S.; Montagnac, G. Tubular clathrin/AP-2 lattices pinch collagen fibers to support 3D cell migration. *Science* **2017**, *356*, 1138–1148.

[174] Subra, C.; Grand, D.; Laulagnier, K.; Stella, A.; Lambeau, G.; Paillasse, M.; De Medina, P.; Monsarrat, B.; Perret, B.; Silvente-Poirot, S. et al. Exosomes account for vesicle-mediated transcellular transport of activatable phospholipases and prostaglandins. *J. Lipid Res.* **2010**, *51*, 2105–2120.

[175] Vlassov, A. V.; Magdaleno, S.; Setterquist, R.; Conrad, R. Exosomes: Current knowledge of their composition, biological functions, and diagnostic and therapeutic potentials. *Biochim. Biophys. Acta-Gen. Subj.* **2012**, *1820*, 940–948.

[176] Kourembanas, S. Exosomes: Vehicles of intercellular signaling, biomarkers, and vectors of cell therapy. *Annu. Rev. Physiol.* **2015**, *77*, 13–27.

[177] Naqvi, S.; Samim, M.; Abdin, M.; Ahmed, F. J.; Maitra, A.; Prashant, C.; Dinda, A. K. Concentration-dependent toxicity of iron oxide nanoparticles mediated by increased oxidative stress. *Int. J. Nanomedinice* **2010**, *5*, 983–989.

[178] Hu, L. Z.; Wickline, S. A.; Hood, J. L. Magnetic resonance imaging of melanoma exosomes in lymph nodes. *Magn. Reson. Med.* **2015**, *74*, 266–271.

[179] Gould, S. J.; Raposo, G. As we wait: Coping with an imperfect nomenclature for extracellular vesicles. *J. Extracell. Vesicles* **2013**, *2*. 20389–20391.

[180] Jovic, M.; Sharma, M.; Rahajeng, J.; Caplan, S. The early endosome: A busy sorting station for proteins at the crossroads. *Histol. Histopathol.* **2010**, *25*, 99–112.

[181] Busato, A.; Bonafede, R.; Bontempi, P.; Scambi, I.; Schiaffino, L.; Benati, D.; Malatesta, M.; Sbarbati, A.; Marzola, P.; Mariotti, R. Magnetic resonance imaging of ultrasmall superparamagnetic iron oxide-labeled exosomes from stem cells: A new method to obtain labeled exosomes. *Int. J. Nanomedicine* **2016**, *11*, 2481–2490.

[182] Busato, A.; Bonafede, R.; Bontempi, P.; Scambi, I.; Schiaffino, L.; Benati, D.; Malatesta, M.; Sbarbati, A.; Marzola, P.; Mariotti, R. Labeling and magnetic resonance imaging of exosomes isolated from adipose stem cells. *Curr. Protoc. Cell Biol.* **2017**, *75*, 1–15.

[183] Zhao, J. Y.; Chen, G.; Gu, Y. P.; Cui, R.; Zhang, Z. L.; Yu, Z. L.; Tang, B.; Zhao, Y. F.; Pang, D. W. Ultrasmall magnetically engineered Ag_2Se quantum dots for instant efficient labeling and whole-body high-resolution multimodal real-time tracking of cell-derived microvesicles. *J. Am. Chem. Soc.* **2016**, *138*, 1893–1903.

[184] Grange, C.; Tapparo, M.; Bruno, S.; Chatterjee, D.; Quesenberry, P. J.; Tetta, C.; Camussi, G. Biodistribution of mesenchymal stem cell-derived extracellular vesicles in a model of acute kidney injury monitored by optical imaging. *Int. J. Mol. Med.* **2014**, *33*, 1055–1063.

[185] Zhu, L.; Dong, D.; Yu, Z. L.; Zhao, Y. F.; Pang, D. W.; Zhang, Z. L. Folate-engineered microvesicles for enhanced target and synergistic therapy toward breast cancer. *ACS Appl. Mater. Interfaces* **2017**, *9*, 5100–5108.

[186] Ridder, K.; Keller, S.; Dams, M.; Rupp, A. K.; Schlaudraff, J.; Del Turco, D.; Starmann, J.; Macas, J.; Karpova, D.; Devraj, K. et al. Extracellular vesicle-mediated transfer of genetic information between the hematopoietic system and the brain in response to inflammation. *PLoS Biol.* **2014**, *12*, e1001874–e1001889.

[187] Feng, D.; Zhao, W. L.; Ye, Y. Y.; Bai, X. C.; Liu, R. Q.; Chang, L. F.; Zhou, Q.; Sui, S. F. Cellular internalization of exosomes occurs through phagocytosis. *Traffic* **2010**, *11*, 675–687.

[188] Nanbo, A.; Kawanishi, E.; Yoshida, R.; Yoshiyama, H. Exosomes derived from epstein-barr virus-infected cells are internalized via caveola-dependent endocytosis and promote phenotypic modulation in target cells. *J. Virol.* **2013**, *87*, 10334–10347.

[189] Christianson, H. C.; Svensson, K. J.; van Kuppevelt, T. H.; Li, J. P.; Belting, M. Cancer cell exosomes depend on cell-surface heparan sulfate proteoglycans for their internalization and functional activity. *Proc. Natl. Acad. Sci. USA* **2013**, *110*, 17380–17385.

[190] Macario, A. J. L.; Cappello, F.; Zummo, G.; de Macario, E. C. Chaperonopathies of senescence and the scrambling of interactions between the chaperoning and the immune systems. *Ann. NY Acad. Sci.* **2010**, *1197*, 85–93.